METRIC/INCH-POUND

KSC-STD-Z-0017
REVISION A

# ENGINEERING ANALYSIS, THERMAL/FLUID, STANDARD FOR

**NOT EXPORT CONTROLLED**
This document has been reviewed by the KSC Export Control Office and it has been determined that it does not meet the criteria for control under the International Traffic in Arms Regulations (ITAR) or Export Administration Regulations (EAR).

*Reference EDR Log #: 11584 NASA KSC Export Control Office, (321) 867-9209*

# ENGINEERING DIRECTORATE

National Aeronautics and
Space Administration

**John F. Kennedy Space Center**

KSC FORM 16-12 (REV. 6/95) PREVIOUS EDITIONS ARE OBSOLETE (CG 11/95)

METRIC/INCH-POUND

KSC-STD-Z-0017
REVISION A

# ENGINEERING ANALYSIS, THERMAL/FLUID, STANDARD FOR

March 29, 2022

## JOHN F. KENNEDY SPACE CENTER, NASA

## RECORD OF REVISIONS/CHANGES

| REV LTR | CHG NO. | DESCRIPTION | DATE |
|---|---|---|---|
| | | Basic issue. | May 8, 2014 |
| A | | Revised spacecraft thermal design margin discussion. Added maximum pressure definitions. Added reference for VAB interior air temperatures. Updated ground and space environmental conditions. Added Appendix F. Miscellaneous changes to reflect new technologies, methodologies and revisions to source documents. | March 29, 2022 |

## CONTENTS

## FIGURES



## TABLES

## ABBREVIATIONS, ACRONYMS, AND SYMBOLS

| | |
|---|---|
| % | percent |
| ° | degree |
| °C | degree Celsius |
| °F | degree Fahrenheit |
| °R | degree Rankine |
| AFT | Applied Flow Technology |
| ANSI | American National Standards Institute |
| ASME | American Society of Mechanical Engineers |
| ASTM | American Society for Testing and Materials |
| atm | atmosphere |
| Btu | British thermal unit |
| CAD | computer-aided design |
| CDR | Critical Design Review |
| CEA | Chemical Equilibrium with Application |
| CFD | computational fluid dynamics |
| DT | design temperature |
| DWG | drawing |
| e.g. | for example |
| ESD | Exploration Systems Development |
| ft | foot |
| g | gram |
| GCI | grid convergence index |
| GFSSP | Generalized Fluid System Simulation Program |
| GSFC | Robert H. Goddard Space Flight Center |
| HDBK | handbook |
| hr | hour |
| in | inch |
| IR | infrared |
| ISA | International Society of Automation |
| J | joule |

| | |
|---|---|
| K | kelvin |
| k | kilo ($1 \cdot 10^3$) |
| KSC | John F. Kennedy Space Center |
| lb | pound |
| $lb_f$ | pound force |
| $lb_m$ | pound mass |
| m | meter |
| m | milli ($1 \cdot 10^{-3}$) |
| MAPTIS | Materials and Processes Technical Information System |
| MAWP | Maximum Allowable Working Pressure |
| Max | maximum |
| MDP | Maximum Design Pressure |
| Min | minimum |
| MLI | multilayered insulation |
| MNL | manual |
| mol | molar |
| MOP | Maximum Operating Pressure |
| MSFC | George C. Marshall Space Flight Center |
| N | newton |
| NA | not applicable |
| NASA | National Aeronautics and Space Administration |
| n/d | nondimensional |
| NIST | National Institute for Standards and Technology |
| Pa | pascal |
| PDR | Preliminary Design Review |
| POAT | predicted operating/acceptance temperature |
| psf | pound per square foot |
| psi | pound per square inch |
| psia | pound per square inch absolute |
| QT | qualification temperature |
| s | second |

| | |
|---|---|
| scfm | cubic foot per minute at standard conditions |
| scms | cubic meter per second at standard conditions |
| SI | International System of Units |
| SINDA/ | |
| FLUINT | Systems Improved Numerical Differencing Analyzer with Fluid Integrator |
| SM | standard manual |
| SPEC | specification |
| ST | survival temperature |
| STD | standard |
| TPSX | Thermal Protection Systems Expert |
| VJ | vacuum-jacketed |
| W | watt |

This page intentionally left blank.

# ENGINEERING ANALYSIS, THERMAL/FLUID, STANDARD FOR

## 1. SCOPE

This document defines the top-level requirements, methods, and boundary conditions that will be applied to all thermal and fluid analyses for systems designed and developed for use at Kennedy Space Center (KSC), as well as for any spacecraft, instruments, and flight experiments designed and developed by KSC. This will include but is not limited to the following topics:

- required documentation,
- analysis guidelines,
- components,
- tubing and piping,
- heat transfer, and
- environments.

## 2. APPLICABLE DOCUMENTS

Acceptable sources of thermophysical properties of fluids and materials are listed in Appendix A.

Additional sources cited by reference number throughout this standard are listed in Appendix B.

The following documents form a part of this document to the extent specified herein. When this document is used for procurement, including solicitations, or is added to an existing contract, the specific revision levels, amendments, and approval dates of said documents shall be specified in an attachment to the Solicitation/Statement of Work/Contract.

### 2.1 Government Documents

| | |
|---|---|
| 545-PG-8700.2.1D | Procedures and Guidelines: Requirements for Thermal Design, Analysis, and Development, NASA GSFC |
| ARC-STD-8070.1 | Space Flight System Design and Environmental Test |

| | |
|---|---|
| KSC-GP-425 | Fluid Fitting Engineering Standards |
| KSC-SPEC-P-0027 | Tubing, Superaustenitic Steel, Corrosion Resistant, UNS N08367 and UNS S31254, Seamed, Bright Annealed, Passivated, Specification for |
| KSC-SPEC-Z-0007 | Tubing, Steel, Corrosion Resistant, Types 304 and 316, Seamless, Annealed, Specification for |
| KSC-SPEC-Z-0008 | Fabrication and Installation of Flared Tube Assemblies and Installation of Fittings and Fitting Assemblies, Specification for |
| KSC-STD-Z-0005 | Pneumatic Ground Support Equipment, Design of, Standard for |
| KSC-STD-Z-0008 | Ground Life Support Systems and Equipment, Design of, Standard for |
| KSC-STD-Z-0009 | Cryogenic Ground Support Equipment, Design of, Standard for |
| MSFC-DWG-20M02540 | Assessment of Flexible Lines for Flow Induced Vibration |
| NASA-HDBK-8739.19-2 | Measuring and Test Equipment Specifications, NASA Measurement Quality Assurance Handbook – Annex 2 |
| NASA-STD-7009 | Standard for Models and Simulations |
| SLS-SPEC-159 | Cross-Program Design Specification for Natural Environments (DSNE) |
| SMC-S-016 | Test Requirements for Launch, Upper-Stage and Space Vehicles |

(Copies of specifications, standards, drawings, and publications required by suppliers in connection with specified procurement functions shall be obtained from the procuring activity or as directed by the Contracting Officer.)

## 2.2 Non-Government Documents

| | |
|---|---|
| ANSI/ISA 75.01.01 | Flow Equations for Sizing Control Valves |

| | |
|---|---|
| ASME B16.9 | Factory-Made Wrought Buttwelding Fittings |
| ASME B31.3 | Process Piping Guide |
| ASME B36.10M | Welded and Seamless Wrought Steel Pipe |
| ASME B36.19M | Stainless Steel Pipe |
| ASME MFC-3M | Measurement of Fluid Flow in Pipes Using Orifice, Nozzle, and Venturi |
| ASME Section VIII, Division 1 | Rules for Construction of Pressure Vessels |
| ASME V&V 20 | Standard for Verification and Validation in Computational Fluid Dynamics and Heat Transfer |
| ASTM B88 | Standard Specification for Seamless Copper Water Tube |
| ASTM MNL 36 | Safe Use of Oxygen and Oxygen Systems: Handbook for Design, Operation, and Maintenance |

## 3. NOMENCLATURE AND DEFINITIONS

$A$ : area (mm$^2$) [in$^2$]

$A_T$ : orifice throat area (m$^2$) [ft$^2$]

$A_{W:}$ : wall area (m$^2$) [ft$^2$]

$A$ : thermal diffusivity (m$^2$/s) [ft$^2$/s]

$C_d$ : orifice and nozzle discharge coefficient (n/d)

$C_{sf}$: surface-fluid constant (n/d)

$C_v$ : valve flow coefficient (n/d)

$c_L$ : specific heat of liquid (J/kg) [Btu/lb$_m$·°R]

$D_{eff}$ : effective diameter (mm) [in]

$D_h$ : hydraulic diameter (mm) [in]

$d_{BL}$ : baseline diameter (mm) [in]

$d_i$ : inner diameter (mm) [in]

$d_1$ : orifice inner diameter (mm) [in]

$d_2$ : pipe inner diameter for orifice calculations (mm) [in]

$f$ : friction factor (n/d)

$\boldsymbol{f_t}$ : friction factor (fully turbulent flow) (n/d)

$\boldsymbol{g}$ : standard gravitational acceleration (9.807 m/s$^2$) [32.174 ft/s$^2$]

$\boldsymbol{g_c}$ : gravitational proportionality constant (1 kg·m/N·s$^2$) [32.174 lb$_m$·ft/lb$_f$·s$^2$]

$\boldsymbol{H_L}$ : head loss (m) [ft]

$\boldsymbol{H}$ : height (m) [ft]

$\boldsymbol{h_b}$ : boiling coefficient (W/m$^2$·°C) [Btu/(hr·ft$^2$·°R)]

$\boldsymbol{i_{fg}}$ : heat of vaporization (J/kg) [Btu/lb$_m$]

$\boldsymbol{J_a}$ : Jakob number (n/d)

$\boldsymbol{K}$ : loss coefficient (n/d)

$\boldsymbol{K_P}$ : dimensionless quantity (n/d)

$\boldsymbol{K_n}$ : loss coefficient for pipe bends other than 90° (n/d)

$\boldsymbol{K_1}$ : upstream loss coefficient (n/d)

$\boldsymbol{K_2}$ : downstream loss coefficient (n/d)

$\mathbf{K_{45°}}$ : loss coefficient for 45° bend or elbow (n/d)

$\boldsymbol{K_{90°}}$ : loss coefficient for 90° bend or elbow (n/d)

$\boldsymbol{K}$ : isentropic exponent (n/d)

$\boldsymbol{k_L}$ : thermal conductivity of liquid (W/m-°C) [Btu/hr·ft·°R]

$\boldsymbol{L}$ : length (mm) [in]

$\dot{m}$ : mass flow rate (kg/s) [lb$_m$/s]

$\boldsymbol{n_{90°}}$ : number of 90° bends

$\boldsymbol{P}$ : pressure (Pa) [psia]

$\boldsymbol{P_c}$ : critical pressure (Pa) [psia]

$\boldsymbol{P_R}$ : rated pressure (Pa) [psia]

$\mathbf{Pr}_{\boldsymbol{L}}$ : Prandtl number of liquid (n/d)

$\boldsymbol{P_S}$ : saturation pressure (Pa) [psia]

$\boldsymbol{P_{SAT}}$ : fluid saturation pressure (Pa) [psia]

$\boldsymbol{P_{STD}}$ : standard fluid pressure (Pa) [psia]

$\boldsymbol{P_1}$ : inlet pressure (Pa) [psia]

$\boldsymbol{P_2}$ : outlet pressure (Pa) [psia]

$\boldsymbol{Q}$ : heat transfer rate (W) [Btu/hr]

$\boldsymbol{Q_R}$ : rated volumetric flow rate (scms) [scfm]

$\boldsymbol{Q_{STD}}$ : volumetric flow rate at standard conditions (scms) [scfm]

$\boldsymbol{Q}$ : boiling heat flux (W/m$^2$)

$\boldsymbol{R}$ : constant of specific gas (N·m/kg·K) [ft·lb$_f$/lb$_m$·°R]

$\boldsymbol{R_e}$ : Reynolds number (n/d)

$\boldsymbol{R_{e_{eff}}}$ : Reynolds number based on effective correction (n/d)

$\boldsymbol{R_{e_{D_h}}}$: Reynolds number based on hydraulic diameter (n/d)

$\boldsymbol{R}$ : radius (mm) [in]

$\boldsymbol{R}$ : latent heat of vaporization (J/kg)

$\boldsymbol{r_a}$ : inside radius of outer pipe for concentric pipes (mm) [in]

$\boldsymbol{r_b}$ : outside radius of inner pipe for concentric pipes (mm) [in]

$\boldsymbol{T_R}$ : rated fluid temperature (K) [°R]

$\boldsymbol{T_{SAT}}$ : fluid saturation temperature (K) [°R]

$\boldsymbol{T_{STD}}$ : standard fluid temperature (K) [°R]

$\boldsymbol{T_W}$ : wall temperature (K) [°R]

$\mathbf{T_1}$ : inlet temperature (K) [°R]

$\boldsymbol{V}$ : flow velocity (m/s) [ft/s]

$\boldsymbol{X_t}$ : pressure differential ratio (n/d)

$\boldsymbol{Y}$ : net expansion factor for compressible flows (n/d)

$\boldsymbol{Z}$ : compressibility factor (n/d)

$\boldsymbol{Z_R}$ : compressibility factor at rated conditions (n/d)

$\boldsymbol{Z_{STD}}$ : standard gas compressibility factor (n/d)

$\boldsymbol{Z_1}$ : compressibility factor at inlet conditions (n/d)

$\boldsymbol{A}$ : absorptivity (n/d)

$\boldsymbol{B}$ : diameter ratio ($d_1/d_2$) for orifice, nozzles, and venturi (n/d)

$\boldsymbol{\Gamma}$ : gas-specific heat ratio (n/d)

$\boldsymbol{\gamma''}$ : specific weight of vapor (N/m$^3$) [lb$_f$/ft$^3$]

$\Delta \boldsymbol{Pr}$ : rated pressure drop (Pa) [psi]

$\boldsymbol{\Delta P}$ : pressure differential (Pa) [psi]

$\boldsymbol{\Delta T}$ : temperature differential (K) [°R]

$\boldsymbol{E}$ : emissivity (n/d); absolute roughness (mm) [in]

$\boldsymbol{Z}$ : correction factor for $D_h$ (n/d)

$\boldsymbol{\Theta}$ : angle of convergence or divergence in enlargements or contractions in pipes (degrees)

$\boldsymbol{\Lambda}$ : thermal conductivity of liquid (W/m·°C)

$\boldsymbol{\mu_L}$ : viscosity of liquid (Pa·s) [$lb_m$/ft·hr]

$\boldsymbol{\rho}$ : density (kg/m$^3$) [$lb_m/ft^3$]

$\boldsymbol{\rho_G}$ : density of vapor (kg/m$^3$) [$lb_m/ft^3$]

$\boldsymbol{\rho_L}$ : density of liquid (kg/m$^3$) [$lb_m/ft^3$]

$\boldsymbol{\rho_R}$ : density at a rated condition (kg/m$^3$) [$lb_m/ft^3$]

$\boldsymbol{\rho_{STD}}$ : density at a standard condition (kg/m$^3$) [$lb_m/ft^3$]

$\boldsymbol{\sigma}$ : surface tension (N/m) [$lb_f$/ft]

$\boldsymbol{\sigma_L}$ : surface tension of liquid (N/m) [$lb_f$/ft]

$\boldsymbol{\upsilon}$ : kinematic viscosity (m$^2$/s) [ft$^2$/s]

$\boldsymbol{\upsilon/a}$ : Prandtl number of liquid (n/d)

$\boldsymbol{\varphi}$ : relative humidity (n/d)

## 4. DOCUMENTATION AND SOFTWARE PACKAGES FOR THERMAL AND FLUID ANALYSIS

This section outlines the requirements for thermal and fluid analysis software packages. The selection of software to be used for a particular project or program shall be coordinated with the lead analyst and is typically defined in the analysis plan.

### 4.1 Incompressible Single-Phase Flow Analysis

A number of software packages are available to analyze fluid networks for which incompressible liquid flow (e.g., water or petroleum product flows) can be assumed. Many of these software packages are capable of only steady-state, single-phase flow analysis and are inappropriate for the analysis of cryogenic liquid flows because these cryogenic flows are frequently operated in near-saturation conditions. An example of a software package appropriate for analysis of incompressible single-phase flows is AFT Fathom. Transient incompressible flow analysis may be accomplished with SINDA/FLUINT or GFSSP.

### 4.2 Gaseous Flow Analysis

A number of software packages are available to analyze fluid networks (e.g., pneumatic systems, environmental control systems, and purges) operating in the gas phase. Though in many cases the ideal gas assumption is appropriate, the high range of operating pressures for KSC systems requires software packages that can account for gas compressibility.

Many of these software packages are capable of only steady-state, single-phase flow analysis and are inappropriate for the analysis of the flow of gases at cryogenic temperatures. An example of a software package appropriate for analysis of noncryogenic gaseous flows is AFT Arrow. Transient compressible flow analysis may be accomplished with SINDA/FLUINT or GFSSP. An AFT gaseous transient solver, xStream is under evaluation by NE-XY.

### 4.3 Water Hammer Analysis

The analysis of fluid line pressure surge, or water hammer, is frequently required. Because water hammer is a transient phenomenon, appropriate surge analysis software is required. An example of a software package appropriate specifically for water hammer analysis is AFT Impulse. General-purpose flow network analysis software with full transient capability, such as SINDA/FLUINT, is also appropriate.

### 4.4 Saturated Flow Analysis

Systems operated at or near saturation conditions, commonly including cryogenic fluid systems, must be analyzed with software capable of multiphase flow calculations in order to accurately capture the behavior of the system. An example of a software package appropriate for analysis of systems operated at or near saturation conditions is SINDA/FLUINT.

### 4.5 Thermal Analysis

Thermal analysis of particular system components can often be performed in conjunction with the analyses described in 4.1 through 4.4. However, situations may arise where three-dimensional thermal analysis may be necessary. A variety of appropriate computer-aided design (CAD)-based analysis packages are available. An example of a software package appropriate for such analysis is Thermal Desktop.

## 5. SOLUTION INDEPENDENCE AND SENSITIVITY

### 5.1 Independent Solutions

All models shall be verified to have produced solutions that are independent of the time step or the number of elements used to make the fluid or thermal analysis model. If adjusting these parameters alters the results, the solution is not independent and is therefore inherently invalid.

#### 5.1.1 Time Step Independence

Time steps for transient solutions shall be decreased or increased to verify that the solution achieved in the computational model is independent of the time step. Only results that have been verified to be independent of the time step are considered valid. A time step independent solution will have no greater than a 1.0% change in any of following: the time to steady state, temperature, pressure, or flow rate of the system being evaluated.

### 5.1.2 Fluid Node Independence

Fluid nodes used in computational models shall be tested for independent solutions. The number of nodes used to represent a fluid system shall be decreased or increased to verify that the solution achieved in the computational model is independent of the number of nodes used. Only results that have been verified to be independent of the number of fluid nodes are considered valid. A fluid node independent solution will have no greater than a 1.0% change in any of the following: the time to steady state, temperature, pressure, or flow rate of the system being evaluated.

### 5.1.3 Thermal Node Independence

Thermal nodes used in computational models shall be tested for independent solutions. The number of nodes used to represent thermal effects shall be decreased or increased to verify that the solution achieved in the computational model is independent of the number of nodes used. Only results that have been verified to be independent of the number of thermal nodes used are considered valid. A thermal node independent solution will have no greater than a 1.0% change in any of the following: the time to steady state, temperature, pressure, or flow rate of the system being evaluated.

### 5.1.4 Radiation Ray Independence

Radiation rays used in computational models shall be tested for independent solutions. The number of rays used shall be decreased or increased to verify that the solution achieved in the computational model is independent of the number of rays used. Only results that have been verified to be independent of the number of rays used are considered valid. A radiation ray independent solution will have no greater than a 1.0% change in temperature of the system being evaluated.

### 5.1.5 Mesh Independence

The size of elements in a computational fluid dynamics (CFD) mesh shall be tested for independent solutions. The number and size of elements shall be decreased or increased to verify that the solution achieved in the computational model is independent of the grid or mesh being used. Only results that have been verified to be independent of the grid or mesh used are considered independent.

## 5.2 Sensitivity Analysis

A sensitivity analysis shall be performed on a model to determine how the input parameters affect the output of the computational model. Different types of sensitivity are described in more detail in NASA-HDBK-8739.19-2.

### 5.2.1 Single-Parameter Sensitivity Analysis

In single-parameter sensitivity analysis, the input parameters are assumed to be independent of one another, and only a single input parameter is changed at a time. The input values that shall be used for each test case are displayed as dots on cubes and are discussed in 5.2.1.1.

#### 5.2.1.1 Two-Level Factorial Sensitivity Analysis

The two-level factorial method can be applied quickly and easily to early computer models. However, its applicability is limited because it can only show linear relationships between input and response values. For this method, three input factors (e.g., $X_1$, $X_2$, and $X_3$) may be varied, each having a maximum and minimum value, which would require a total of $2^3 = 8$ test cases. If these three factors were depicted in a three-dimensional plot, they would form a cube, as shown in Figure 1.

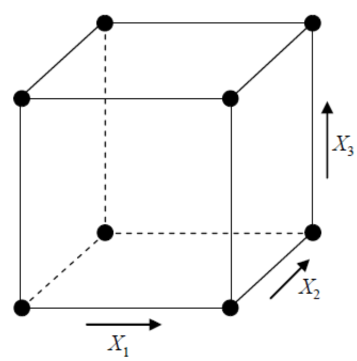


*From NASA-HDBK-8739.19-2.*

**Figure 1. Two-Level $2^3$ Factorial Input Parameter Cube**

#### 5.2.1.2 Three-Level Factorial Sensitivity Analysis

The three-level factorial method uses three input factors (e.g., $X_1$, $X_2$, and $X_3$) that may be varied. Each input factor has a maximum, minimum, and nominal value. This method can produce quadratic curves but requires a total of $3^3 = 27$ test cases to complete. If these three factors were depicted in a three-dimensional plot, they would form a cube, as shown in Figure 2. This figure excludes the point at the center of each face and the point at the center of the box, but these seven additional points shall be incorporated into the analysis.

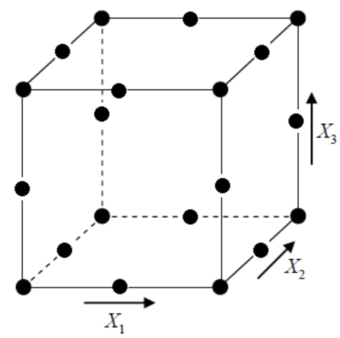


*From NASA-HDBK-8739.19-2.*

**Figure 2. Three-Level $3^3$ Factorial Input Parameter Cube**

#### 5.2.1.3 Box-Behnken Sensitivity Analysis

The Box-Behnken method uses three input factors (e.g., $X_1$, $X_2$, and $X_3$) that may be varied. Each input factor has a maximum, minimum, and nominal value. This method is a simpler version of the three-level factorial method and requires a total of 15 test cases to complete. If these three factors were depicted in a three-dimensional plot, they would form a cube, as shown in Figure 3.

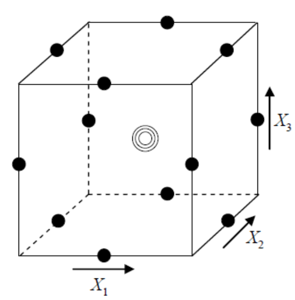


*From NASA-HDBK-8739.19-2.*

**Figure 3. Box-Behnken Input Parameter Cube**

### 5.2.2 Multiple-Parameter Sensitivity Analysis

In multiple-parameter sensitivity analysis, all input parameters are assigned a probability distribution, or uncertainty, that is propagated throughout the model, using a Monte Carlo simulation. This type of method accounts for input parameter interactions. This type of sensitivity analysis can be time-consuming and shall be completed as part of a Preliminary Design Review (PDR) deliverable.

## 5.3 Grid Convergence Index (GCI)

GCI shall be performed in accordance with Section 2 of ASME V&V 20 in order to test for the convergence of structured and unstructured CFD grids and meshes.

#### 5.3.1 Safety Factor for Structured Mesh

When GCI is used, a safety factor of 1.25 shall be applied to all structured mesh in accordance with Section 2 of ASME V&V 20.

#### 5.3.2 Safety Factor for Unstructured Mesh

When GCI is used, a safety factor of 3.0 shall be applied to all unstructured mesh in accordance with Section 2 of ASME V&V 20.

### 5.4 Sensitivity Coefficients and Importance Factors

Sensitivity coefficients for input parameters to any computational model shall be determined using the methods outlined in Section 3 of ASME V&V 20.

Importance factors shall be used to determine which parameters will have the greatest effect on the solution of a computational model. These factors shall be determined using the methods outlined in Appendix B of ASME V&V 20.

### 5.5 Errors and Uncertainties

Errors and uncertainties between numerical simulations and experimental values shall be determined using the methods outlined in Section 1 of ASME V&V 20.

## 6. BOUNDING CONDITIONS AND DESIGN MARGINS

### 6.1 Bounding Cases

Thermal and fluid systems need to be evaluated to ensure that they will meet the requirements for the project within prescribed bounding conditions. In general, these are the worst-case thermal and fluid conditions that can be expected for the system.

#### 6.1.1 Ground System Thermal Bounding Conditions

The worst-case parameters for ground system thermal analysis are outlined in Table 1.

**Table 1. Worst-Case Parameters for Ground Thermal Analysis**

| Hot Operating Condition | Cold Operating Condition |
|---|---|
| Max environmental fluxes (diffuse and direct) | Min environmental fluxes (diffuse and direct) |
| Max indoor/outdoor ambient temperature | Min indoor/outdoor ambient temperature |
| Interface conductance that will produce the hottest temperatures | Interface conduction that will produce the coldest temperatures |
| Max $\alpha$/Min $\varepsilon$ of thermal coatings (degraded values) | Min $\alpha$, Max $\varepsilon$ of thermal coatings |

| Hot Operating Condition | Cold Operating Condition |
|---|---|
| Min blanket $\varepsilon^*$ if the heat flow is out,<br>Max if heat flow is in | Max blanket $\varepsilon^*$ if the heat flow is out,<br>Min if heat flow is in |
| Min frost accumulation on surface for insulation,<br>Max for vaporization | Max frost accumulation on surface for insulation,<br>Min for vaporization |
| Min ice accumulation on surface for insulation,<br>Max for vaporization | Max ice accumulation on surface for insulation,<br>Min for vaporization |
| $\alpha$ = absorptivity   $\varepsilon$ = emissivity   $\varepsilon^*$ = effective emissivity | |

### 6.1.2 Spacecraft Thermal Bounding Conditions

The worst-case parameters for spacecraft thermal analysis are discussed in 545-PG-8700.2.1D and are outlined in Table 2.

**Table 2. Worst-Case Parameters for Spacecraft Thermal Analysis**

| Parameter | Hot Operating Condition | Cold Operating Condition | Hot Survival Condition | Cold Survival Condition |
|---|---|---|---|---|
| **Environmental Fluxes (Solar, Albedo, IR)** | Maximum for science data collecting orbit | Minimum for science data collecting orbit | Maximum during mission | Minimum during mission |
| **Thermo-Optical Properties (of Thermal Coatings)** | α: Maximum<br>ε: Minimum (degraded values) | α: Minimum<br>ε: Maximum (non-degraded values) | α: Maximum<br>ε: Minimum (degraded values) | α: Minimum<br>ε: Maximum (non-degraded values) |
| **Power Dissipation (see note below)** | Maximum orbital average | Minimum | Maximum average survival mode | Minimum average survival mode |
| **Interface Conductance** | produce the hottest temperatures | produce the coldest temperatures | produce the hottest temperatures | produce the coldest temperatures |
| **MLI ε*** | Minimum if the heat flow is out, Maximum if heat flow is in | Maximum if the heat flow is out, Minimum if heat flow is in | Minimum if the heat flow is out, Maximum if heat flow is in | Maximum if the heat flow is out, Minimum if heat flow is in |
| **Solar Cells: Efficiency (η): Solar Absorptance (α):** | Minimum η Maximum α (for maximum solar cell temperature) | Maximum η Minimum α (for minimum solar cell temperature) | Minimum η Maximum α (for maximum solar cell temperature) | Maximum η Minimum α (for minimum solar cell temperature) |
| **Bus Voltage** | Maximum operational (heater dissipation) | Minimum operational (heater dissipation) | Maximum (heater dissipation) | Minimum (heater dissipation) |
| **Failure Modes** | Assess credible modes | | | |
| | $\alpha$ = absorptivity   $\varepsilon$ = emissivity   $\varepsilon^*$ = effective emissivity | | | |
| Note: Use for Steady-State Analysis: For transient analyses use power versus time if applicable. | | | | |
| | *From 545-PG-8700.2.1D.* | | | |

### 6.1.3 Fluid System Bounding Conditions

Fluid densities, particularly for gases and cryogenic liquids, are highly variable. Therefore, fluid systems shall be evaluated at the highest possible input pressure and the lowest possible input temperature, as well as the opposite case. System-specific bounding conditions shall be applied as described below as necessary.

#### 6.1.3.1 Backpressure in Vent Systems

Vent systems shall be sized to provide minimum backpressure, consistent with required venting flow rates. In no case shall the backpressure interfere with the proper operation of safety relief devices or pneumatically operated devices. A design analysis shall be performed to ensure that excessive backpressure will not occur in vent systems, as specified in KSC-STD-Z-0005 and ASME Section VIII, Division 1, Paragraph UG-156(i).

#### 6.1.3.2 Gaseous System Velocity Constraint

Velocity of gaseous systems other than oxygen should be kept under Mach 0.2 whenever possible as a noise reduction measure. Generally, flow velocities under Mach 0.2 will avoid flow-induced vibration concerns in flexible metal hose, per KSC-STD-Z-0005, but FIV calculations shall still be performed. See Section 6.2.1.

##### 6.1.3.2.1 Gaseous Oxygen Velocity Constraint

The velocity of gaseous oxygen during normal flow conditions shall be kept under 30.48 meters per second (m/s) (100 feet per second [ft/s]), as specified in ASTM MNL 36.

#### 6.1.3.3 Gaseous Oxygen Pressure Drop Constraint

The pressure difference across a filter or other component shall not be allowed to exceed 3%. Pressure differences greater than 3% absolute can ignite particles in oxygen-enriched systems [1].

### 6.1.4 Contingency Scenarios

Operational criteria may require that operational contingency scenarios be evaluated.

## 6.2 Flow Device Constraints and Considerations

This section outlines certain constraints introduced by particular flow devices that shall be addressed during analysis of a compressible fluid system, as well as any considerations that shall be addressed in the analysis. In this section, *shall* denotes a constraint on the system, and *should* denotes a consideration or recommendation for the system.

### 6.2.1 Flexible Metal Hose

Flow-induced vibration shall be addressed in any design that uses convoluted, unlined bellows or flexible metal hoses, as specified in MSFC-DWG-20M02540.

### 6.2.2 Pressure Relief Devices

The relieving capability of a relief device shall be equal to or greater than the maximum flow capability of the upstream pressure regulator or pressure source. Setpoint and overpressure allowance requirements shall be as specified in ASME B31.3 and ASME Section VIII, Division 1. All sources of overpressure must be considered, including:

- Pressure regulator failure
- Pressure relief valve failure
- Superimposed backpressure due to upstream component failure

Relief device inlet losses, any set pressure tolerances, and superimposed backpressure shall be considered as specified in KSC-STD-Z-0005 to ensure that any such effects will not adversely affect the relieving capacity of the proper operation of the relief device. The effects of hydraulic head should also be considered as necessary when considering a relief device.

#### 6.2.2.1 Relief Valve

Pressure relief valves for cryogenic systems shall also reseat at greater than 85% of their set pressure, as specified in KSC-STD-Z-0009.

For all relief valves, it is recommended that (3%) be subtracted from the design pressure level to establish the upper bound of the relief valve set point which leaves (7%) margin in the system for Relief Valve sizing.

#### 6.2.2.2 Fusible Plug/Burst Disk

A fusible plug or burst disk assembly shall comply with the following requirements, as specified in KSC-STD-Z-0008.

- The burst disk shall burst at the pressure vessel’s maximum allowable working pressure plus 10% to 30%.

- The discharge flow rate, upon rupture of the burst disc, shall not be less than the flow rate of the nearest downstream relief valve.

#### 6.2.2.3 Maximum Pressure Definitions

ASME Section VIII, Division 1 Paragraph UG-98 specifies that a vessel’s maximum allowable working pressure (MAWP) is the maximum pressure at which a relief valve protecting the vessel must be set to guard against system rupture. ASME B31.3 Paragraph 322.6.3a terms this same maximum pressure as the Design Pressure, or Maximum Design Pressure (MDP).

Under normal, or steady-state operating conditions, a system may have a maximum operating pressure or maximum working pressure that is lower than MAWP or MDP, depending on system functionality requirements. ISO 5598, *Fluid power systems and components—Vocabulary* is useful for relating pressure definitions to each other.

### 6.2.3 Regulators

In pressure regulators, the ratio of the upstream pressure to the downstream pressure should not exceed 5. This practice increases control of the pressure and flow and reduces problems in sizing a pressure-relieving device. In cases where a higher turndown ratio is required, the effects of the turndown ratio shall be analyzed and documented, as specified in KSC-STD-Z-0005 Section 4.5.1. The pressure regulator shall comply with the following additional requirements as specified in KSC-STD-Z-0008 for ground life support systems:

- The pressure reduction (outlet) shall not be less than 2% of the supply pressure (inlet) for a one-stage regulator.
- The accuracy of the pressure regulator shall be within 10% of its specified setting throughout the specified pressure supply (inlet) range.

#### 6.2.3.1 Pressure-Regulating Circuits

The design of pressure-regulating circuits shall be predicated upon a detailed analysis of the system requirements, including those downstream of the design interface. This analysis shall consider but shall not be limited to the following items, as specified in KSC-STD-Z-0005:

- required accuracy of regulation,
- minimum and maximum flow rates expected,
- reliability required, and
- operational requirements.

#### 6.2.3.2 Flow Rate Contingency Factor

Pressure-regulating circuits shall be designed with the capability to maintain the required outlet pressure within required tolerances at a flow rate not less than 25% above the normal system requirements, as specified in KSC-STD-Z-0005.

### 6.2.3.3 Regulator Flow Scenarios

Regulators used in pneumatic systems shall be evaluated under two different flow scenarios: nominal, and low-density conditions. A regulator shall not be used if it cannot deliver the required flow under any one of these conditions.

#### 6.2.3.3.1 Nominal Conditions

Run the model, using the nominal expected pressure and temperature as inlet conditions. All losses should be at their nominal values. Verify that the pressure drop and flow through the system are within acceptable limits.

#### 6.2.3.3.2 Low-Density Conditions

Run the model, using the lowest expected inlet pressure and highest expected inlet temperature as inlet conditions. System losses should be at the highest possible value (e.g. minimum orifice CdA; minimum tube ID; maximum component Cv and K values). Verify that the pressure drop and flow through the system under low-density conditions are within acceptable limits.

## 6.3 Design Margins

Design margins shall be used in the thermal analysis of a system in order to help the system achieve at least a 95% confidence level. A summary sheet of all thermal/fluid design margins is incorporated in Appendix C.

### 6.3.1 Design Margins for Fluid Flow

Design margins shall be applied to the flow rates of all fluid flow systems. These margins shall be the same for the design and the analysis of ground support equipment and spacecraft systems.

#### 6.3.1.1 Design Margins for Compressible-Gas Flow

Design margins shall be applied to the flow rates of all compressible-gas systems. These margins shall be applied to the nominal flow required for the system and shall not be smaller than the margins outlined in this section. Design margins shall vary depending on the maturity of the design, as outlined in Appendix C.

According to KSC-STD-Z-0005 and 6.2.3.2, a flow margin of ±25% shall be used on nominal desired flow of the system to determine high-flow and low-flow conditions. A safety factor of 2.5 was applied to this value to obtain the maximum design margin to be used during design and analysis. The safety factor was established by the chief engineer, and deviation requires the chief engineer’s approval.

#### 6.3.1.2 Design Margins for Incompressible-Liquid Flow

Design margins shall be applied to the flow rates of all incompressible-liquid or cryogenic systems. These margins shall be applied to the nominal flow required for the system and shall not be smaller than the margins outlined in this section. Design margins shall vary depending on the maturity of the design, as outlined in Appendix C.

Historical data on pumped cryogenic systems has shown that flow rates may vary by ±25%. A safety factor of 2.0 was applied to this value to obtain the maximum design margin to be used during design and analysis. The safety factor applied was determined by the chief engineer.

### 6.3.2 Design Margins for Two-Phase Fluid Quality

Design margins shall be applied to the flow rates of all fluid systems where two-phase fluid quality is a concern, such as cryogenic systems. These margins shall be the same for the design and the analysis of ground support equipment and spacecraft systems. When maximum quality is required by the system, the quality margin that most constrains the system design shall be applied to that requirement. If the maximum quality allowed in a system is 0.0, then a margin shall be applied to the fluid temperature to keep the liquid in a subcooled state. Design margins shall vary depending on the maturity of the design, as outlined in Appendix C.

### 6.3.3 Thermal Design Margins for Ground Systems

Design margins shall be applied to the design and analysis of all ground systems. The correct margins to apply shall be whichever margins challenge the design the most. Design margins applied to the heat load of the system shall be evaluated first, since they are a higher-order boundary condition that shall challenge the system the most. For example, a system susceptible only to vacuum shall be evaluated by using radiation heat load design margins, whereas a heat exchanger or condenser shall be evaluated by using convection heat load design margins. Design margins shall vary depending on the maturity of the design, as outlined in Appendix C.

### 6.3.4 Thermal Design Margins for Spacecraft

Design margins shall be applied to all spacecraft environmental temperatures and heat rates. The correct margins to apply will depend on whether the spacecraft system is cryogenic or noncryogenic, as well as whether the system has active or passive thermal control.

a. A passive thermal control device or system is defined as having any of the following characteristics as outlined in [2]:

   (1) constant-conductance or diode heat pipes,

   (2) hard-wired heaters (either fixed-resistance or variable-resistance, such as autotrace or positive-temperature-coefficient thermistors),

   (3) thermal storage devices (phase-change or sensible-heat),

(4) thermal insulation (multilayer insulation [MLI], foams, or discrete shields),

(5) radiators (fixed, articulated, or deployable) with louvers, or

(6) surface finishes (coatings, paints, treatments, second-surface mirrors).

b. An active thermal control device or system is defined as having any of the following characteristics as outlined in [2]:

(1) variable-conductance heat pipes,

(2) heat pumps and refrigerators,

(3) stored-coolant subsystems,

(4) heaters with commandable, mechanical, or electronic controllers,

(5) capillary pumped loops,

(6) pumped fluid loops, or

(7) thermoelectric coolers.

#### 6.3.4.1 Thermal Design and Test Margins for Noncryogenic Systems

This section discusses the design and test margins that shall be used in the design and analysis of noncryogenic systems for spacecraft. Limits and margins that shall be assigned to temperature values are illustrated in Figure 4.

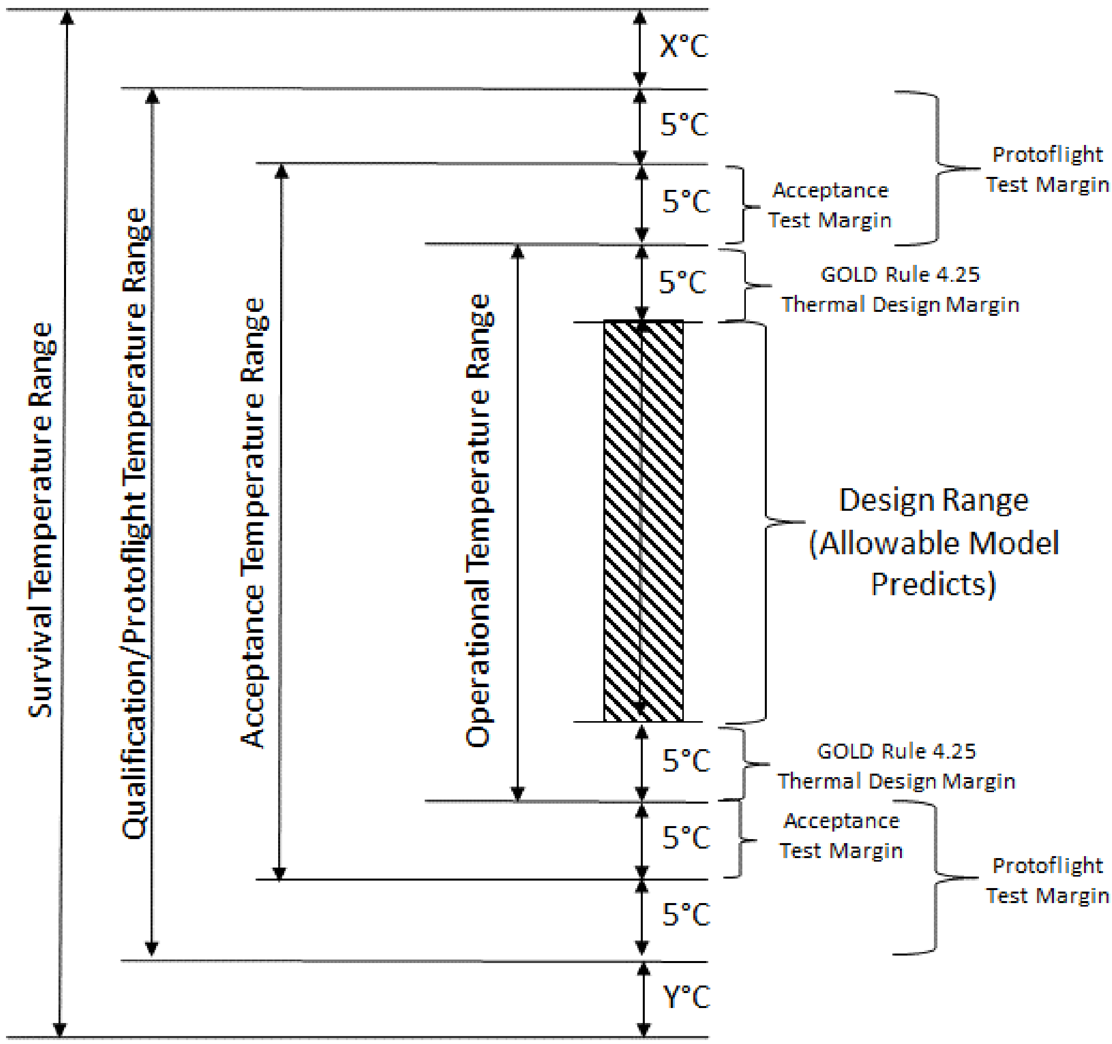


*From 545-PG-8700.2.1D.*

**Figure 4. Spacecraft Thermal Margins**

*Notes:*
*- Cold design limit can equal cold operational limit if heater controlled with 30% duty cycle margin*
*- Acceptance limits apply only if identical units have been previously qualified and flown successfully through similar lifetime and environment.*
*- Cold/Hot turn on must be at least as wide as the qualification limits*
*- Survival limits must be at least as wide as the qualification limits; typically, X = 5°C, Y =10°C*
*- Subsystem/System testing may limited by flight heater(s) setpoints*
*- Some programs/projects will recommend the margins in ARC-STD-8070.1. These are essentially interchangeable.*

Heaters shall be sized such that the hardware does not drop below temperature limits if the heater is at the minimum voltage and at 70% duty cycle (30% margin) under worst-case environmental conditions. (545-PG-8700.2.1D)

#### 6.3.4.2 Thermal Design Margins for Cryogenic Systems

This section discusses the design margins that shall be used in the design and analysis of cryogenic systems for spacecraft. Limits and margins that shall be assigned to temperature values are outlined in Table 3. In addition, a 15% margin will be applied to any project-approved power dissipation values. For actively controlled systems (e.g., pumped fluid loops), a heat load margin of 25% shall be used as specified in [2], in lieu of the minimum expected temperature.

If the temperature is actively being maintained below 120 Kelvin (K) (216 degrees Rankine [°R]), then design margins shall vary depending on the maturity of the design. Table 3 identifies the design margins for passive and active cryogenic systems.

**Table 3. Thermal Margins for Passive Cryogenic Spacecraft Systems**

| | | Uncorrelated Model, 95% Confidence Level | Correlated Model, 95% Confidence Level |
|---|---|---|---|
| Heat load margin (%) | | 50% | 25% |
| Predicted temperature (K/°R) | | Temperature Margin (K) | Temperature Margin (K) |
| >203 K | (365.4 °R) | 17 | 11 |
| 186–203 K | (334.8–365.4 °R) | 16 | 10 |
| 168–185 K | (302.4–333.0 °R) | 15 | 9 |
| 150–167 K | (270.0–300.6 °R) | 14 | 8 |
| 132–149 K | (237.6–268.2 °R) | 13 | 7 |
| 114–131 K | (205.2–235.8 °R) | 11 | 6 |
| 96–113 K | (172.8–203.4 °R) | 9 | 5 |
| 78–95 K | (140.4–171.0 °R) | 8 | 4 |
| 60–77 K | (108.0–138.6 °R) | 6 | 3 |
| 42–59 K | (75.6–106.2 °R) | 4 | 2 |
| 23–41 K | (21.6–73.8 °R) | 2 | 1 |
| <23 K | (<21.6 °R) | 1 | 1 |

*From* [2].

## 7. COMPONENT INPUTS

This section discusses the methods for determining the relevant flow characteristics of components to be used in the analyzed system, including components in KSC control drawings or vendor control drawings. All component characteristics shall be represented by calculating the loss coefficient at the component's rated condition for its rated fluid commodity, unless otherwise specified for an individual component type.

## 7.1 Standard Conditions

Standard conditions in the English system are assumed to be $P_{STD}$ = 14.7 pounds per square inch absolute (psia) and $T_{STD}$ = 519.67 °R (101.325 kilopascals [kPa] and 15.6 °C).

## 7.2 Component Documentation

The manufacturer, model, and part numbers for all components shall be identified in the analysis documentation. All components shall be modeled using KSC specification or vendor drawing data, when available. All components shall be modeled using the resistance coefficient *K* for that component at its rated conditions and working fluid.

## 7.3 Loss Coefficient

Use of the loss (or resistance) coefficient (*K*) is preferred for fluid network calculations. When only the flow coefficient ($C_v$) is available, Eq. 1 can be used to determine the loss coefficient for components. This equation determines the loss coefficient as a function of the flow coefficient and internal diameter in inches. This equation is valid for compressible and incompressible fluids that do not have high viscosity.

$$K = \frac{890.3 d_i^{\,4}}{C_v^{\,2}} \qquad \textbf{Eq. 1}$$

*Derived from Equation 2-11 of* [3], *page 2-9.*
*Replace 890.3 with 0.002139 for equations that use the International System of Units (SI).*

For straight piping and tubing, the loss coefficient can be determined by using the friction factors outlined in 7.4, along with Eq. 2. The turbulent friction factor may replace the laminar friction in Eq. 2 for turbulent flow conditions.

$$K = f \cdot \frac{L}{d_i} \qquad \textbf{Eq. 2}$$

*From Equation 2-4 of* [3], *page 2-7.*

## 7.4 Friction Factor

### 7.4.1 Friction Factor in Circular Pipes

In most cases, the approximate friction factor may be determined by the Moody diagram, found on pages A-24 through A-26 of [3]. For more explicit results, the friction factor may be calculated. For laminar flow ($R_e < 2000$), the friction factor is found by Eq. 3.

$$f = \frac{64}{R_e} \qquad \textbf{Eq. 3}$$

*From Equation 1-18 of* [3], *page 1-6.*

Flow in the turbulent region ($R_e$ > 4000) may be found by the Colebrook equation, Eq. 4:

$$\frac{1}{\sqrt{f}} = -2.0\log\left(\frac{\varepsilon}{3.7d_i} + \frac{2.51}{R_e\sqrt{f}}\right) \qquad \textbf{Eq. 4}$$

*From Equation 1-20 of* [3], *page 1-7.*

Eq. 4 requires an iterative solution for *f*, which may be accomplished using programs such as Microsoft Excel or MathCAD. Alternatively, a form of the Colebrook equation applicable for fully turbulent flow (Eq. 5) or the approximations given on page 1-7 of [3] may be used.

$$f_t = \frac{0.25}{\left[log\frac{\left(\frac{\varepsilon}{d_i}\right)}{3.7}\right]^2} \qquad \textbf{Eq. 5}$$

*From Equation 2-8 of* [3], *page 2-9.*

### 7.4.2 Friction Factor in Concentric Cylinders With Concentric Annuluses

For flow through the annulus of two concentric cylinders, the friction factors are larger than standard flow through a circular pipe. For calculating the friction factor through the annulus, the hydraulic diameter is used in place of the actual diameter. The hydraulic diameter is found by Eq. 6.

$$D_h = 2\cdot(r_a - r_b) \qquad \textbf{Eq. 6}$$

*From Equation 6-75 of* [4], *page 381.*

The dimensionless term, ζ, is a correction factor for the hydraulic diameter that can be found from Eq. 7.

$$\zeta = \frac{(r_a - r_b)^2\cdot(r_a{}^2 - r_b{}^2)}{r_a{}^4 - r_b{}^4 - \frac{(r_a{}^2 - r_b{}^2)^2}{\ln\left(\frac{r_a}{r_b}\right)}} \qquad \textbf{Eq. 7}$$

*From Equation 6-76 of* [4], *page 381.*

The effective Reynolds number is needed to determine the friction factor and is found by Eq. 8. The Reynolds number based on the hydraulic diameter will need to be determined using the actual flow area to determine the average velocity.

$$R_{e_{eff}} = \frac{1}{\zeta}\cdot R_{e_{D_h}} \qquad \textbf{Eq. 8}$$

*From Equation 6-77 of* [4], *page 381.*

For a laminar flow, the friction factor in concentric annular flow is found by Eq. 9.

$$f = \frac{64}{R_{e_{eff}}} \qquad \textbf{Eq. 9}$$

*From Equation 6-77 of* [4], *page 381.*

For turbulent flow in a concentric annulus, the friction factor may be found by using the Colebrook equation, Eq. 4, with minor changes. The hydraulic Reynolds number shall be used in place of the Reynolds number. Also, the effective diameter replaces the regular diameter, which is found using Eq. 10.

$$D_{eff} = \frac{D_h}{\zeta} \qquad \textbf{Eq. 10}$$

*From Equation 6-77 of* [4], *page 381.*

The updated form of the Colebrook equation for concentric annular flow is shown in Eq. 11.

$$\frac{1}{\sqrt{f}} = -2.0\log\left(\frac{\frac{\epsilon}{D_{eff}}}{3.7} + \frac{2.51}{R_{e_{D_h}}\sqrt{f}}\right) \qquad \textbf{Eq. 11}$$

*From Example 6.14 of* [4], *pages 381-382.*

Alternatively, an adjusted form of Eq. 5, using the effective diameter instead of the diameter, may be tried and compared with iterative results from Eq. 11.

### 7.5 Pressure Loss

The pressure loss may be determined easily once the loss coefficient and friction factors are determined. Applying these known values to Eq. 12, the general form of the Darcy Equation, will calculate the loss of static pressure head, also known as head loss.

$$H_L = K \cdot \frac{v^2}{2 \cdot g} \qquad \text{Eq. 12}$$

*From Equation 2-3 of* [3], *page 2-7.*

The head loss may then be applied to Eq. 13 to determine the differential pressure loss.

$$\Delta P = H_L \cdot \rho \cdot g \qquad \text{Eq. 13}$$

*From Equation 11.2 of* [4], *page 751.*

If the head loss was not determined before the differential pressure drop was solved, then Eq. 14 may be used to calculate the differential pressure drop directly. The turbulent friction factor may be used in lieu of the laminar friction factor in Eq. 14 when applicable.

$$\Delta P = f \cdot \frac{L}{d_i} \cdot \frac{v^2}{2 \cdot g} \cdot \frac{\rho}{144} \qquad \text{Eq. 14}$$

*From Equation 1-17 of* [3], *page 1-6.*
*Replace 144 with 1 for SI units.*

### 7.6 Components

In the majority of cases, analysis software will provide acceptable correlations (upon verification) for losses due to components. When hand calculations are performed or when software correlations are not available, the remaining sections apply.

#### 7.6.1 Regulators and Valves

The loss coefficient for all valves, check valves, and regulators shall be determined from either KSC component specification drawings or vendor drawings whenever possible. Flow coefficients shall be converted to loss coefficients via Eq. 2.

When KSC component specifications or vendor drawings are not available for a particular valve, the methods outlined for flow without attached fittings in ANSI/ISA 75.01.01 shall be used to determine the flow coefficient, which will then be converted to loss coefficient for modeling use. The listed applicability check for each equation shall also be performed to determine if the use of that equation is acceptable and shall be noted in the analysis documentation. ANSI/ISA 75.01.01 contains equations applicable for both compressible and incompressible fluids.

When ANSI/ISA 75.01.01 is used to determine the flow coefficient of a valve that is to be used in compressible fluid service, a pressure differential ratio ($X_t$) shall be specified. A nominal value shall be selected from Table 2 of ANSI/ISA 75.01.01, based on the type of valve being used. In addition, a high and low value of 0.3 and 0.9 shall be used to determine the minimum and maximum range for determining whether a component is choking.

A spreadsheet shall be available supplying loss coefficients for both compressible and incompressible components. [5]

#### 7.6.2 Filters

The loss coefficient for filters shall be determined from either KSC component specification drawings or vendor drawings whenever possible. Flow losses through a filter are typically given in terms of a maximum pressure drop at a given flowrate. This may be incorporated into the Darcy Equation as outlined in Section 7.5 to determine loss coefficient. Flow through a gas filter is typically specified in terms of volumetric flow at standard conditions, e.g. SCFM. For convenience, Eq. 15, was derived from the Darcy equation from [3] to determine the loss coefficient for gaseous filters. The derivation is shown in Appendix D.

A spreadsheet [6] is available on the Design and Analysis Wiki page [7] to assist NASA and contractor personnel with these calculations.

$$K = \left(\frac{60}{144}\right)^2 \cdot \frac{g \cdot \pi^2 \cdot R \cdot P_R \cdot \Delta P_R \cdot Z_{STD}{}^2 \cdot T_{STD}{}^2 \cdot d_{BL}{}^4}{8 \cdot P_{STD}{}^2 \cdot Q_R{}^2 \cdot Z \cdot T_R} \qquad \textbf{Eq. 15}$$

*Derived by Stephen Van Genderen from equations in* [3].
*Replace* $(60/144)^2$ *with* $(1/1000000)^2$ *for SI units.*

### 7.6.3 Orifices and Cavitating Flows

Orifice behavior for gases can be determined using the following equations.

$$\dot{m} = C_d A_T \rho \sqrt{2 g_c \frac{\gamma}{\gamma - 1} Z_1 R T_1 \left[\left(\frac{P_2}{P_1}\right)^{\frac{2}{\gamma}} - \left(\frac{P_2}{P_1}\right)^{\frac{\gamma+1}{\gamma}}\right]} \qquad \textbf{Eq. 16}$$

*Equation 3.8.2.3b of* [8].

$$\dot{m} = 144 \cdot C_d A_T P_1 \sqrt{\frac{g_c \gamma}{Z_1 R T_1}\left(\frac{2}{\gamma + 1}\right)^{\frac{\gamma+1}{\gamma-1}}} \qquad \textbf{Eq. 17}$$

*Equation 3.8.2.3g of* [8].
*Remove the 144 for SI units.*

Use Eq. 16 when $\frac{P_2}{P_1} > \frac{P_c}{P_1}$. Use Eq. 17 when $\frac{P_2}{P_1} < \frac{P_c}{P_1}$. Use Eq. 18 to determine the ratio of critical pressure to inlet pressure to be used in the above-mentioned conditions.

$$P_c = P_1 \left(\frac{2}{\gamma + 1}\right)^{\frac{\gamma}{\gamma-1}} \qquad \textbf{Eq. 18}$$

*Equation 3.3.8.9d of* [8].

For cavitated liquid flow (as in a cavitating venturi or liquid orifice), Eq. 19 shall be used.

$$\dot{m} = C_d A_T \sqrt{\frac{144 \cdot 2 g_c \rho \left(P_1 - P_s\right)}{\left(1 - \beta^4\right)}} \qquad \textbf{Eq. 19}$$

*From Equations 4-5 and 4-6 of* [3].
*Remove the 144 for SI units.*

Common engineering practice has been to assume a $C_d$ of 0.6 for orifices. More recent work has developed some empirical correlations for $C_d$ for orifices, nozzles, and venturis. These are found in [1] as Equations 4-7 through 4-13. If $C_d$ is known for an orifice plate or for an ISA 1932 or a long-radius nozzle, the loss coefficient may be found as follows:

$$K = \left[ \frac{\sqrt{1-\beta^4 \cdot \left(1-C_d^2\right)}}{C_d \cdot \beta^2} - 1 \right]^2 \qquad \textbf{Eq. 20}$$

*From ASME MFC-3M, Equation 2-10, page 26.*

A relationship between equivalent sharp-edged orifice diameter and flow coefficient is given by Eq. 21.

$$d_1 = 0.2364\sqrt{C_v}X \qquad \textbf{Eq. 21}$$

*From* [9] and (SVG).

Where X=1 for liquids at small or negligible orifice beta ratios. For gases under choked, ideal gas conditions, X must be calculated as:

$$X = \sqrt{\frac{\sqrt{1-\left(\frac{2}{\gamma+1}\right)^{\frac{2\gamma}{\gamma-1}}}}{\sqrt{\gamma\left(\frac{2}{\gamma+1}\right)^{\frac{\gamma+1}{\gamma-1}}}}} \qquad \textbf{Eq. 22}$$

*From* [9] and (SVG).

A spreadsheet [10] shall be available to determine loss coefficients for both compressible and incompressible orifices under choked and unchoked conditions. The discharge coefficient for subcritical, unchoked flows for both compressible and incompressible fluids is a function of the pipe Reynolds number. Since the Reynolds number changes based on the fluid flow rate, the equations to calculate the flow coefficient for an unchoked orifice shall be used only in hand calculations.

For pneumatics applications, the standard KSC orifices referenced as KC175 and KC176 in GP-425 provide choked orifice flowrates with tolerances for select gases. Orifice CdAs may be calculated using this information and Eq. 17.

#### 7.6.3.1 Discharge Coefficients for Orifice Plates

As stated in 7.6.3, the discharge coefficient for orifice plates has been determined to be a function of the Reynolds number from the upstream pipe. Further information on this relationship is discussed in ASME MFC-3M, which is summarized in [3]. The relationships outlined in Eq. 23 through Eq. 24 are limited to use under the following conditions.

a. For orifice plates with corner or with D and ½ D pressure taps:

(1) $d_1 \geq 12.5$ mm (0.5 in)

(2) 50 mm (2 in) $\leq d_2 \leq$ 1000 mm (40 in)

(3) $0.10 \leq \beta \leq 0.75$

(4) $R_e \geq 5000$ for $0.10 \leq \beta \leq 0.56$

(5) $R_e \geq 16{,}000\beta^2$ for $\beta > 0.56$

b. For orifice plates with flange taps:

(1) $d_1 \geq$ 12.5 mm (0.5 in)

(2) 50 mm (2 in) $\leq d_2 \leq$ 1000 mm (40 in)

(3) $0.10 \leq \beta \leq 0.75$

(4) $R_e \geq 5000$ and $R_e \geq 170\beta^2 d_2$ ($d_2$, millimeters) ($R_e \geq 4318\beta^2 d_2$ [$d_2$, inches)

c. For gases, $0.80 < (P_2/P_1) < 1.00$

d. $\Delta P \leq$ 250348.6 Pa (36.31 pounds per square inch [psi])

The discharge coefficient for orifice plates is determined by Eq. 23. The ratio $L_1$ is the distance from the upstream tap to the upstream orifice plate face, divided by the pipe diameter. The ratio $L_2$ is the distance of the downstream tap from the downstream orifice plate face, divided by the pipe diameter.

$$C_d = 0.5961 + 0.0261\beta^2 - 0.216\beta^8 + 0.000521\cdot\left(\frac{10^6\cdot\beta}{R_e}\right)^{0.7}$$
$$+\left(0.0188 + 0.0063\cdot\left(\frac{19000\beta}{R_e}\right)^{0.8}\right)\cdot\beta^{3.5}\cdot\left(\frac{10^6}{R_e}\right)^{0.3}$$
$$+\left(0.043 + 0.080e^{-10L_1} - 0.123e^{-7L_1}\right)\cdot\left(1 - 0.11\cdot\left(\frac{19000\beta}{R_e}\right)^{0.8}\right)\cdot\frac{\beta^4}{1-\beta^4}$$
$$-0.031\cdot\left(\left(\frac{2L_2}{1-\beta}\right) - 0.8\cdot\left(\frac{2L_2}{1-\beta}\right)^{1.1}\right)\cdot\beta^{1.3}$$

*From ASME MFC-3M, Equation 2-4, page 25.*

**Eq. 23**

Values for $L_1$ and $L_2$ to be used in Eq. 23 are as follows:

- Corner taps: $L_1 = L_2 = 0$
- D and ½ D pressure taps: $L_1 = 1$, $L_2 = 0.47$

- Flange taps: $L_1 = L_2 = 1/d_2$

If the inner diameter ($d_2$) of the pipe is less than 71.12 mm (2.8 in), the term shown as Eq. 24 shall be added onto Eq. 23.

$$+0.011 \cdot (0.75 - \beta) \cdot (2.8 - d_2) \qquad \textbf{Eq. 24}$$

*From ASME MFC-3M, Equation 2-5, page 25.*
*Divide $d_2$ by 25.4 for SI units.*

### 7.6.3.2 Expansion Factor for Orifice Plates

The expansibility factor for compressible flow through an orifice plate may be needed for some unchoked conditions and is determine by Eq. 25. The isentropic exponent may be replaced with the gas specific heat ratio for an ideal gas.

$$Y = 1 - \left(0.351 + 0.256\beta^4 + 0.93\beta^8\right) \cdot \left[1 - \left(\frac{P_2}{P_1}\right)^{\frac{1}{k}}\right] \qquad \textbf{Eq. 25}$$

*From ASME MFC-3M, Equation 2-6, page 25.*

### 7.6.3.3 Discharge Coefficient for Flow Nozzles

The discharge coefficient for flow nozzles is dependent on the Reynolds number of the flow. Further information on this relationship is discussed in ASME MFC-3M, which is summarized in [2].

a. For ISA 1932 flow nozzles, the discharge coefficient is given by Eq. 26. For ISA 1932 flow nozzles, Eq. 26 is used only when the following conditions are satisfied.

   (1) 50 mm (2 in) $\leq d_2 \leq$ 500 mm (2 in)

   (2) $0.30 \leq \beta \leq 0.80$

   (3) $7\ (10^4) \leq R_e \leq 1\ (10^7)$ for $0.30 \leq \beta \leq 0.44$

   (4) $2\ (10^4) \leq R_e \leq 1\ (10^7)$ for $0.44 \leq \beta \leq 0.80$

$$C_d = 0.9900 - 0.2262\beta^{4.1} - \left(0.00175\beta^2 - 0.0033\beta^{4.15}\right) \cdot \left(\frac{10^6}{R_e}\right)^{1.15} \qquad \textbf{Eq. 26}$$

*From ASME MFC-3M, Equation 3-6, page 52.*

b. For long-radius flow nozzles, the discharge coefficient is given by Eq. 27 and must satisfy the following conditions to be acceptable for use.

(1) 50 mm (2 in) $\leq d_2 \leq$ 630 mm (25 in)

(2) $0.20 \leq \beta \leq 0.80$

(3) $1\ (10^4) \leq R_e \leq 1\ (10^7)$

(4) $\varepsilon/d_2 \leq 3.2\ (10^{-4})$

$$C_d = 0.9965 - 0.00653\beta^{0.5}\left(\frac{10^6}{R_e}\right)^{0.5} \qquad \textbf{Eq. 27}$$

*From ASME MFC-3M, Equation 3-12, page 55.*

c. For venturi nozzles, the discharge coefficient is given by Eq. 28 and must satisfy the following conditions to be acceptable for use.

(1) 65 mm (2.5 in) $\leq d_2 \leq$ 500 mm (20 in)

(2) $d_1 \geq$ 50 mm (2 in)

(3) $0.316 \leq \beta \leq 0.775$

(4) $1.5\ (10^5) \leq R_e \leq 2\ (10^6)$

$$C_d = 0.9858 - 0.196\beta^{4.5} \qquad \textbf{Eq. 28}$$

*From ASME MFC-3M, Equation 3-16, page 57.*

### 7.6.3.4 Discharge Coefficients for Venturi Meters

The discharge coefficient for venturi meters is dependent on the method of manufacturing. The values for these methods are listed here, but analysts are advised to cite the source of this information. See ASME MFC-3M, Sections 4-4.5.2, 3, and 4 (page 73), for more detailed information.

a. "As-Cast" convergent section: $C_d = 0.984$

(1) 100 mm (4 in) $\leq d_2 \leq$ 1200 mm (48 in)

(2) $0.30 \leq \beta \leq 0.75$

(3) $2\ (10^5) \leq R_e \leq 6\ (10^6)$

b. Machined convergent section: $C_d = 0.995$

(1) 50 mm (2 in) $\leq d_2 \leq$ 250 mm (10 in)

(2) $0.30 \leq \beta \leq 0.75$

(3) $2\ (10^5) \leq R_e \leq 6\ (10^6)$

c. Rough-welded convergent section: $C_d = 0.985$

(1) 100 mm (4 in) $\leq d_2 \leq$ 1200 mm (48 in)

(2) $0.30 \leq \beta \leq 0.75$

(3) $2\ (10^5) \leq R_e \leq 6\ (10^6)$

### 7.6.3.5 Expansion Factor for Flow Nozzles and Venturi Meters

The expansibility factor for compressible flow through a flow nozzle or venturi meter may be needed for some nonchoked conditions and is determined by Eq. 29. The isentropic exponent may be replaced with the gas specific heat ratio for an ideal gas.

$$Y = \left\{ \left( \frac{k \cdot \left( \frac{P_2}{P_1} \right)^{2/k}}{k-1} \right) \cdot \left( \frac{1-\beta^4}{1-\beta^4 \cdot \left( \frac{P_2}{P_1} \right)^{2/k}} \right) \cdot \left[ \frac{1-\left( \frac{P_2}{P_1} \right)^{(k-1)/k}}{1-\left( \frac{P_2}{P_1} \right)} \right] \right\}^{0.5} \qquad \textbf{Eq. 29}$$

*From ASME MFC-3M, Equation 4-3, page 73.*

### 7.6.4 Relief Valves

Relief valves are pressure-relieving devices that have an internal orifice and shall be sized for the maximum flow rate possible through an orifice under choked flow conditions. The equations used to determine the flow rate through a relief valve are outlined in 7.6.3.

### 7.6.4.1 Relief Valve Sizing for Cryogenic Systems

Relief valve for cryogenic service shall be able to expel gas at a higher flow rate than can be vaporized inside a vacuum-jacketed (VJ) section. Sizing for cryogenic relief valves is a complicated process and shall be calculated using the following assumptions.

- The VJ section has no thermal resistance.
- The cryogenic fluid is saturated at the relief valve set pressure.

- The heat flux is composed of direct and diffuse solar radiation.
- The heat flux shall be for hottest day of the year.
- The worst-case temperature for the relief valve area is (70 °C) (158 °F).
- The outer VJ pipe shall have an absorptivity of 1.0.

A spreadsheet [11] shall be available to size cryogenic system relief valves based on the maximum direct and diffuse solar radiation a VJ line will experience. Heat leak from connected cryogenic lines can be added to the total heat entering the VJ section.

#### 7.6.4.2 Relief Valve Sizing for Pneumatic Systems

Relief valves for pneumatic service shall be able to expel gas at a higher flow rate than can be delivered by a failed, fully open, upstream regulator. A spreadsheet shall be available to size pneumatic system relief valves based on the failure of the upstream regulator [5]. In addition, regulator failure scenarios shall be evaluated in modeling tools that are approved for pneumatic system analysis.

Two major cases, No Upstream Losses and All Upstream Losses, shall be evaluated to verify that the flow rate is within the rated capability of the relief valve and that the tubing or piping between the regulator and relief valve is large enough to prevent overpressurization of the system. The stagnation pressure immediately downstream of each regulator shall not exceed 110% of the system or vessel maximum allowable working pressure for the corresponding relief valve in any of the cases. The methodology for evaluation of these cases is described in Appendix F.

### 7.6.5 Pumps

#### 7.6.5.1 Centrifugal Pumps

Centrifugal pumps are considered to be head-generating pumps used for large flows and are the more commonly used pumps. Centrifugal pumps shall have a performance curve of the pump’s pressure change versus flow rate for the commodity being analyzed. The inlet and outlet diameters, pump speed, and mechanical and hydraulic efficiencies shall also be provided. The mechanical and hydraulic efficiencies may be represented by a single or total efficiency.

#### 7.6.5.2 Positive-Displacement Pumps

Positive-displacement pumps are flow-generating pumps that displace a fixed amount of fluid per shaft revolution. Positive-displacement pumps shall have a performance curve of the pump’s flow rate versus pressure change for the commodity being analyzed. The following shall also be provided: inlet and outlet diameters; volumetric displacement per revolution; and volumetric, mechanic, and hydraulic efficiencies. The mechanical and hydraulic efficiencies may be represented by a single or total efficiency. The volumetric efficiency shall be provided as a separate value from both the mechanical and hydraulic efficiencies.

### 7.6.6 Flow-Induced Vibration

Flow-induced vibrations for flexible hoses shall be calculated in accordance with MSFC-DWG-20M02540.

### 7.6.7 Elbows and Bends

All flow losses from elbows and bends shall be accounted for in an analysis. Typically, all elbows in cryogenic systems are actual bends, not sudden changes in direction. Elbows shall be modeled as pipe bends unless otherwise directed.

The ratio of bend radius to inner diameter is determined by using ASME B16.9 for pipe bends or KSC-SPEC-Z-0008 for tubing bends. The loss coefficient for 90° bends is shown in Table 4. To determine the loss coefficient for bends other than 90°, use Eq. 30.

**Table 4. Loss Coefficient for 90° Bends and Elbows**

| | | | | | | |
|---|---|---|---|---|---|---|
| $r/d$ | 1 | 1.5 | 2 | 3 | 4 | 6 |
| $K_{90°}$ | $20f_t$ | $14f_t$ | $12f_t$ | $12f_t$ | $14f_t$ | $17f_t$ |
| $r/d$ | 8 | 10 | 12 | 14 | 16 | 20 |
| $K_{90°}$ | $24f_t$ | $30f_t$ | $34f_t$ | $38f_t$ | $42f_t$ | $50f_t$ |

*From the table in* [3], *page A-30.*

$$K_n = \left(n_{90°} - 1\right) \cdot \left(0.25 \cdot \pi \cdot f_t \cdot \frac{r}{d} + 0.5 \cdot K_{90°}\right) + K_{90°} \qquad \textbf{Eq. 30}$$

*From* [3], *page A-30.*

The loss coefficient is determined by Eq. 31 for a 90° elbow and Eq. 32 for a 45° elbow, substituting as appropriate.

$$K_{90°} = 30 \cdot f_t \qquad \textbf{Eq. 31}$$

*From* [3], *for Standard Elbows, page A-30.*

$$K_{45°} = 16 \cdot f_t \qquad \textbf{Eq. 32}$$

*From* [3], *for Standard Elbows, page A-30.*

#### 7.6.7.1 Tees and Wyes

Recent work in the behavior of tees and wyes has shown them to be much more complicated than previously thought. For preliminary work, Figures 2-14 through 2-17 of [3] shall be used. More detailed analyses shall follow the procedure outlined beginning on page 2-14 of [3].

#### 7.6.7.2 Area Changes

The loss coefficient through area changes in pipes or tubes are determined as follows:

Gradual contraction is defined as $\theta \leq 45°$ and shall be determined from Eq. 33.

$$K_1 = 0.8 \cdot \sin\frac{\theta}{2} \cdot \left(1-\beta^2\right) \qquad \textbf{Eq. 33}$$

*From Equation 2-26 of* [3], *page 2-11.*

Sudden contraction is defined as 45°< $\theta \leq 180°$ and shall be determined from Eq. 34.

$$K_1 = 0.5 \cdot \sqrt{\sin\frac{\theta}{2}} \cdot \left(1-\beta^2\right) \qquad \textbf{Eq. 34}$$

*From Equation 2-27of* [3], *page 2-11.*

Gradual enlargement is defined as $\theta \leq 45°$ and shall be determined from Eq. 35.

$$K_1 = 2.6 \cdot \sin\frac{\theta}{2} \cdot \left(1-\beta^2\right)^2 \qquad \textbf{Eq. 35}$$

*From Equation 2-24 of* [3], *page 2-11.*

Sudden enlargement is defined as 45°< $\theta \leq 180°$ and shall be determined from Eq. 36.

$$K_1 = \left(1-\beta^2\right)^2 \qquad \textbf{Eq. 36}$$

*From Equation 2-25 of* [3], *page 2-11.*

If the downstream loss coefficient is desired in place of the upstream loss coefficient, then it shall be determined by using Eq. 37.

$$K_2 = \frac{K_1}{\beta^4} \qquad \textbf{Eq. 37}$$

*From Equation 2-19 of* [3], *page 2-11.*

#### 7.6.7.3 Additional Losses

Any losses not covered in this section shall be applied as a loss coefficient.

## 8. PIPING AND TUBING INPUTS

This section discusses the methods and inputs necessary to represent pressure and flow losses in an analyzed system. These methods shall be applied to both piping and tubing that will be analyzed in the system.

## 8.1 Piping and Tubing Roughness

The pipe roughness shall be taken into account during all calculations for a piping system. The absolute roughness values of commonly used materials are listed in Table 5.

**Table 5. Absolute Roughness Values for Commonly Used Materials**

| Material (Source) | Absolute Roughness mm | (ft) |
|---|---|---|
| AL6XN (KSC-SPEC-P-0027) | 0.0008 | (0.000003) |
| Stainless steel [4] | 0.002 | (0.000007) |
| Invar/iron [4] | 0.046 | (0.00015) |
| Brass/copper [4] | 0.002 | (0.000007) |

## 8.2 Piping and Tubing Wall Thickness

Required pipe thickness shall be determined in accordance with ASME B31.3 Paragraphs 304.1 and 304.2.

All outer diameters, inner diameters, thicknesses, and tolerances of pipe walls shall be in accordance with the correct standards for that type of piping or tubing material, as listed in Table 6.

**Table 6. Applicable Standards for Piping and Tubing Wall Thickness**

| Material | Applicable Standard |
|---|---|
| AL6XN | KSC-SPEC-P-0027 |
| Stainless steel | ASME B36.19M |
| Invar/iron | ASME B36.10M |
| Steel | ASME B36.10M |
| Copper | ASTM B88 |
| Stainless-steel tubing | KSC-SPEC-Z-0007E |

## 8.3 Lengths

For friction losses to be accounted for accurately, the analysis shall include all pipe and tubing lengths. Meandering runs shall not be simplified.

## 8.4 Elevation

The effects of changes in elevation of piping or tubing runs on fluid and thermal properties shall be evaluated in order to provide the most accurate results.

# 9. HEAT TRANSFER

This section provides the methods and boundary conditions used to determine heat transfer calculations.

## 9.1 Material Properties

Temperature-dependent material properties outlined in Appendix A shall be used for all heat transfer calculations.

## 9.2 Fluid Properties

Fluid properties that cause variances in temperature or pressure, outlined inAppendix A, shall be used for all heat transfer calculations.

## 9.3 Optical Properties

### 9.3.1 Acceptable Sources of Optical Properties

Optical properties shall be obtained from test data whenever possible. Information for initial values is available from one of the following databases: Materials and Processes Technical Information System (MAPTIS) or Thermal Protection System Expert (TPSX). Reference [12] is also a widely accepted source for optical properties of several materials and insulations. The absorptivity and emissivity of common materials and insulations are listed in Table 7.

**Table 7. Optical Properties of Common Materials and Insulations**

| Material (Source) | Solar Absorptivity | IR Emissivity |
|---|---|---|
| 304 Stainless Steel (MAPTIS-II) | 0.54 | 0.87 |
| 316 Stainless Steel (MAPTIS-II) | 0.540 | 0.870 |
| Aluminum [12] | 0.170 | 0.100 |
| Double-Sided Aluminized Kapton [12] | 0.140 | 0.050 |
| Double-Sided Aluminized Mylar [12] | 0.140 | 0.050 |
| Nextel 312 [13] | 0.140 | 0.88 |
| 6061-T6 (MAPTIS-II) | NA | 0.2–0.33 |
| Copper (MAPTIS-II) | 0.7 | 0.78 |
| Titanium 6AL-4V (MAPTIS-II) | 0.5 | 0.68 |
| Carbon Steel (MAPTIS-II) | 0.54 | 0.87 |
| BX-250 (MAPTIS-II) | NA | 0.9 |
| NCFI22-65 (MAPTIS-II) | NA | 0.9 |

## 9.4 Ground Environmental Conditions

Environmental conditions, such as the ambient temperatures, shall be as defined in SLS-SPEC-159 and as defined below.

### 9.4.1 Ground Interior-Air Temperatures at KSC

The ambient interior temperatures used for heat transfer calculations shall be $T_{MAXIMUM}$ = 27 °C (80 °F) and $T_{MINIMUM}$ = 15 °C (60 °F).

Under extreme internal conditions for a maximum of 1 hour, the temperature values used shall be $T_{MAXIMUM}$ = 40 °C (104 °F) and $T_{MINIMUM}$ = 11 °C (52 °F).

#### 9.4.1.1 Vehicle Assembly Building Interior Air Temperatures

Ambient Vehicle Assembly Building interior temperatures used for heat transfer calculations shall be $T_{MAXIMUM}$ = 35 °C (95 °F) and $T_{MINIMUM}$ = 4 °C (39.2 °F). See NASA TM-2014-218335.

### 9.4.2 Ground Exterior-Air Temperatures at KSC

The ambient exterior temperatures used for heat transfer calculations shall be $T_{MAXIMUM}$ = 38 °C (100.4 °F) and $T_{MINIMUM}$ = –6 °C (21.2 °F), as defined in SLS-SPEC-159 Section 3.1.5. Section 3.1.5 also defines hot and cold diurnal temperature profiles.

### 9.4.3 Ground Interior Relative Humidity at KSC

The interior relative humidity used for heat transfer calculations shall be $\varphi_{MINIMUM}$ = 30% and $\varphi_{MAXIMUM}$ = 70% at the temperatures specified in 9.4.1, with a nominal value of $\varphi_{NOMINAL}$ = 55%.

### 9.4.4 Ground Exterior Humidity at KSC

Exterior humidity shall be evaluated in accordance with SLS-SPEC-159 Section 3.1.7.

### 9.4.5 Ground Wind Velocities at KSC

Ground wind velocities shall be in accordance with SLS-SPEC-159 Table 3.1.3-4, Table 3.1.3-5, or Table 3.1.3-6, as appropriate.

### 9.4.6 Ground Thermal Energy Environment at KSC

Ground Thermal Energy values shall be in accordance with SLS-SPEC-159 Section 3.1.4.

## 9.5 Space Environmental Conditions for Earth Orbit

Space environmental conditions for Earth orbit shall be taken from SLS-SPEC-159, or as noted below.

### 9.5.1 Deep-Space Temperature

For all Earth orbit analyses involving heat transfer, a deep-space temperature of 2.7 K (4.86 °R) shall be used.

### 9.5.2 Solar Constant

Solar-constant values for Earth orbit analyses shall be in accordance with SLS-SPEC-159 Section 3.3.9.1.1.

### 9.5.3 Albedo Factor

Albedo factor values for Earth orbit analyses shall be in accordance with SLS-SPEC-159 Section 3.3.9.2.

### 9.5.4 Earth Outgoing Longwave Radiation

Values for outgoing longwave radiation (OLR) for Earth orbit analyses shall be in accordance with SLS-SPEC-159 Section 3.3.9.2.

## 9.6 Space Environmental Conditions for Lunar Orbit

Environmental conditions for lunar orbit shall be in accordance with SLS-SPEC-159 Sections 3.3.9 and 3.4.6, as applicable.

## 9.7 Correlations

### 9.7.1 Empirical Correlations

Empirical correlations are very common in the study of heat transfer, particularly with respect to convection. The source of empirical correlations, as well as any applicable validity restrictions, shall be documented. Whenever possible, multiple correlation calculations shall be performed, with the most conservative valid result dominating.

### 9.7.2 Kutateladze Boiling Correlation Correction

When calculations for nucleate boiling are performed, the Kutateladze equation shall be used. This method as applied to cryogenic fluids is discussed in [14]. A correction for this equation has been provided by Randall F. Barron and is attached in Appendix E. The three main equations used in this correlation are outlined below; however, Appendix E shall be consulted for the correct units and meanings of all variables.

The Jakob number ($J_a$) used is determined by using Eq. 38.

$$J_a = \frac{c_L \cdot \left(T_W - T_{SAT}\right)}{i_{fg}} \qquad \textbf{Eq. 38}$$

*From Equation 4-26 of* [14]*, page 164.*

The dimensionless parameter $K_P$ is determined by using Eq. 39.

$$K_P = \frac{P_{SAT} \cdot 144}{\sqrt{\left(g / g_c\right) \cdot \sigma_L \left(\rho_L - \rho_G\right)}} \qquad \textbf{Eq. 39}$$

*From Equation 4-25 of* [14]*, page 164.*
*Remove the 144 for SI units.*

Finally, the heat flux determined by the Kutateladze correlation is calculated by rearranging the derivation shown in Appendix E, which is displayed here as Eq. 40.

$$\frac{Q}{A_W} = \left( \frac{J_a \cdot 0.0007}{Pr_L^{\,0.65} \cdot \left( \frac{\rho_G}{\rho_L \cdot K_P} \right)^{0.7}} \right)^{10/3} \cdot \frac{\mu_L \cdot i_{fg}}{\sqrt{\frac{\sigma_L \cdot g_c}{g \cdot (\rho_L - \rho_G)}}} \qquad \textbf{Eq. 40}$$

*From Equation 4-24 of* [14], *page 164, and corrected in Appendix E.*

## 9.8 Frost and Ice Formation

When cryogenic systems with noninsulated lines are analyzed, the effects of frost or ice formation shall be taken into account. Simple methods of frost formation analysis are available in SINDA/FLUINT and from other sources. Since frost and ice can significantly affect the performance for a system, worst-case conditions, as defined in 6.1, shall be analyzed. Modeling frost effects with a constant heat rate or heat flux value is not recommended.



| Custodian: | Preparing Activity: |
|---|---|
| NASA – John F. Kennedy Space Center<br>Kennedy Space Center, Florida 32899 | John F. Kennedy Space Center<br>Engineering Directorate |

# APPENDIX A. REFERENCES FOR THERMOPHYSICAL PROPERTIES OF FLUIDS AND MATERIALS

Fluid and material properties to be used in the analysis of fluid or thermal systems shall be in accordance with this document. Acceptable sources of material properties are the National Institute for Standards and Technology (NIST), the Thermal Protection Systems Expert (TPSX), MatWeb, and the Materials and Processes Technical Information System (MAPTIS). Acceptable sources of fluid properties are CRTech Property files, NIST's REFPROP database, and Chempak (AFT analysis only).

a. Fluid property references are listed here in the order of preference:

(1) NIST REFPROP,

(2) CRTech Fluid Property Files,

(3) Chemical Equilibrium with Application (CEA),

(4) CEA 2, and

(5) Chempak (single-phase fluids only).

b. Material property references are listed here in the order of preference:

(1) NIST Material Properties,

(2) MAPTIS,

(3) TPSX, and

(4) MatWeb.

This page intentionally left blank.

## APPENDIX B. SPECIFIC REFERENCES

The following references contain supplemental information to guide the user in the application of this standard.

[1] E. Forsyth, "Fundamentals of Oxygen Systems Design & Analysis: Oxygen Safety Training Course Series," 2010.

[2] M. Donabedian, Spacecraft Thermal Control Handbook Volume 2: Cryogenics, American Institute of Aeronautics and Astronautics, Inc., 2003.

[3] Crane, Flow of Fluids Through Valve, Fittings and Pipe. Technical Paper No. 410, Stamford: Crane Company, 2018.

[4] F. M. White, Fluid Mechanics, 5th Edition, New York: McGraw-Hill, 2003.

[5] S. Van Genderen, "Regulator and Relief Valve Sizing Spreadsheet," [Online]. Available: https://sp.ksc.nasa.gov/ne/da/fluids/Shared%20Documents/Wiki/Fluid%20Analysis/Regulator_and_Relief_Valve_Sizing.xlsx.

[6] S. Van Genderen, "Filter_K_Value Calculation_Spreadsheet," [Online]. Available: https://sp.ksc.nasa.gov/ne/da/fluids/Shared%20Documents/Wiki/Fluid%20Analysis/Filter_K_Value_Calculation.xlsx.

[7] S. Anthony, "Pneumatic System Design Analysis," [Online]. Available: https://sp.ksc.nasa.gov/ne/da/fluids/Fluids%20Wiki/Pneumatic%20System%20Design%20Analysis.aspx.

[8] TRW, Aerospace Fluid Component Designer's Handbook, Volume 1, Edwards: Air Force Rocket Propulsion Laboratory, 1970.

[9] Circle Seal Controls, "Engineering Data," Circle Seal Controls, [Online]. Available: http://www.circle-seal.com/products/technical_data/engdata.pdf. [Accessed 26 January 2012].

[10] S. Van Genderen, "GP_425 Spec Orifice Flow Analysis Calibration," [Online]. Available: https://sp.ksc.nasa.gov/ne/da/fluids/Shared%20Documents/Wiki/Fluid%20Analysis/GP_425%20Spec%20Orifice%20Flow%20Analysis%20Calibration_001_UPDATED_20MAY2021.xlsx.

[11] J. Congiardo, "LH2_LO2_ReliefValveCalcs_100prct_REBUILT," [Online]. Available: https://sp.ksc.nasa.gov/ne/da/fluids/Shared%20Documents/Wiki/Fluid%20Analysis/LH2_LO2_ReliefValveCalcs_100prct_REBUILT.xlsx.

[12] D. G. Gilmore, Spacecraft Thermal Control Handbook Volume 1: Fundamental Technologies, American Institute of Aeronautics and Astronautics, Inc., 2002.

[13] 3M Corporation, "Nextel Ceramic Textiles Technical Notebook," [Online]. Available: http://multimedia.3m.com/mws/mediawebserver?mwsId=SSSSSufSevTsZxtUnxme4Y_ZevUqevTSevTSevTSeSSSSSS--&fn=Nextel_Tech_Notebook_11.04.pdf. [Accessed 24 May 2013].

[14] R. F. Barron, Cryogenic Heat Transfer, Philadelphia: Taylor & Francis, 1999.

[15] T. M. Flynn, J. W. Draper and J. J. Roos, "The Nucleate and Film Boiling Curve of LIquid Nitrogen at One Atmosphere," *Advances in Cryogenic Engineering,* vol. 7, pp. 539-545, 1962.

[16] TRW, Aerospace Fluid Component Designers' Handbook Volume 2, Edwards: Air Force Rocket Propulsion Laboratory, 1970.

# APPENDIX C. THERMAL/FLUID DESIGN MARGINS

## C.1 Thermal Design Margins for Spacecraft

Design Margins for Cryogenic Passive Systems (Radiators, Insulation, Thermal Storage Devices)

| Cryogenic Passive | Concept | 30% or PDR | 60% | 90% or CDR |
|---|---|---|---|---|
| Uncorrelated Model | ±17 °C (30.6 °F) | ±17 °C (30.6 °F) | ±17 °C (30.6 °F) | ±17 °C (30.6 °F) |
| Correlated Model | ±11 °C (19.8 °F) | ±11 °C (19.8 °F) | ±11 °C (19.8 °F) | ±11 °C (19.8 °F) |

*Values are for 95% probability of success.*
*Note: Do not use both margins together. Cryogenic design margins shall be used when the temperature will be maintained below 360 °R (200K).*

### C.1.1 Design Margins for Active Systems (Pumped Fluid Loops, Stored-Coolant Subsystems, Fluids in Motion)

| Active Systems | Concept | 30% or PDR | 60% | 90% or CDR |
|---|---|---|---|---|
| Noncryogenic Heat Load Margin | ±30% | ±30% | ±30% | ±30% |
| Cryogenic Heat Load Margin | ±50% | ±45% | ±35% | ±30% |

*Values for cryogenic systems are for 95% probability of success.*

## C.2 Thermal Design Margins for Ground Systems

| | Concept | 30% or PDR | 60% | 90% or CDR |
|---|---|---|---|---|
| Surface Temperature Margin | ±9.44 °C (17 °F) | ±9.44 °C (17 °F) | ±2.78 °C (5 °F) | ±2.78 °C (5 °F) |

or

| | Concept | 30% or PDR | 60% | 90% or CDR |
|---|---|---|---|---|
| Radiation Heat Load Margin | ±50% | ±45% | ±35% | ±30% |
| Convection Heat Load Margin | ±50% | ±45% | ±30% | ±15% |
| Conduction Heat Load Margin | ±50% | ±45% | ±30% | ±15% |

*Note: Do not use both margins together. Use whichever margin challenges the design to the greatest extent.*

## C.3 Design Margins for Two-Phase Fluid Quality

If quality (maximum percentage of vapor) is a design requirement, use the following margins.

| | Concept | 30% or PDR | 60% | 90% or CDR |
|---|---|---|---|---|
| Quality Margin | ±33% | ±33% | ±20% | ±10% |

*For example, if the requirement is to provide a maximum of 6% quality, then the system design shall be for 4% quality through the 30% review.*

If quality (maximum percentage of vapor) is required to be zero, then the margin is on subcooling.

| | Concept | 30% or PDR | 60% | 90% or CDR |
|---|---|---|---|---|
| Subcooling (°F) | –13.33 °C (8 °F) | –13.33 °C (8 °F) | –14.44 °C (6 °F) | –15 °C (5 °F) |
| Subcooling Temperature Multiplier | 2.0 | 2.0 | 1.5 | 1.25 |

*For example, design the system to provide twice the required subcooling, up to the 30% review.*

## C.4 Design Margins for Fluid Flow Rate

### C.4.1 Incompressible (Liquid) Flow

| | Concept | 30% or PDR | 60% | 90% or CDR |
|---|---|---|---|---|
| Flow Rate Margin | ±50% | ±50% | ±35% | ±25% |

*Note: Apply to nominal flow values.*

### C.4.2 Compressible (Gas) Flow

| | Concept | 30% or PDR | 60% | 90% or CDR |
|---|---|---|---|---|
| Flow Rate Margin | ±50% | ±50% | ±30% | ±20% |

*Note: Apply to nominal flow values.*

## APPENDIX D. DERIVATION OF EQ. 15

Eq. 15 in 7.6.2 is derived via the Darcy equation:

$$H_L = K\frac{v^2}{2g} \qquad \textbf{Eq. A}$$

*From* [3], *Equation 1-16.*

Substituting,

$$\Delta P_R = \rho_R g H_L \qquad \textbf{Eq. B}$$

*As obtained from steady flow energy equation.*

and rearranging gives

$$K = \frac{2\Delta P_R}{\rho_R v^2} \qquad \textbf{Eq. C}$$

Converting velocity to mass flow gives

$$K = \frac{2\Delta P_R}{\rho_R\left(\dfrac{\dot{m}}{\rho_R A}\right)^2} = \frac{2\Delta P_R \rho_R A^2}{\dot{m}^2} \qquad \textbf{Eq. D}$$

Because the filter flow rate is given in cubic feet per minute at standard conditions (scfm), mass flow must be converted using the ideal gas law with compressibility for standard conditions:

$$Q_{STD} = \frac{\dot{m}}{\rho_{STD}} = \frac{\dot{m}}{\dfrac{P_{STD}}{RT_{STD}Z_{STD}}} = \frac{\dot{m}RT_{STD}Z_{STD}}{P_{STD}} \qquad \textbf{Eq. E}$$

Substituting Eq. E into Eq. D gives

$$K = \frac{2\Delta P_R \rho_R A^2}{\dfrac{Q_{STD}^2 P_{STD}^2}{R^2 T_{STD}^2 Z_{STD}^2}} = \frac{2\Delta P_R \rho_R A^2 R^2 T_{STD}^2 Z_{STD}^2}{Q_{STD}^2 P_{STD}^2} \qquad \textbf{Eq. F}$$

Converting rated density to rated pressure and temperature via the ideal gas law with compressibility gives

$$K = \frac{2\Delta P_R \dfrac{P_R}{RT_R Z_R} A^2 R^2 T_{STD}^2 Z_{STD}^2}{Q_{STD}^2 P_{STD}^2} = \frac{2\Delta P_R P_R A^2 R T_{STD}^2 Z_{STD}^2}{Q_{STD}^2 P_{STD}^2 T_R Z_R} \qquad \textbf{Eq. G}$$

Finally, applying conversion factors and rearranging gives the following:

$$K = \left(\frac{60}{144}\right)^2 \cdot \frac{g_c \pi^2 R P_R \Delta P_R Z_{STD}^2 T_{STD}^2 d_{BL}^4}{8 P_{STD}^2 Q_{STD}^2 Z_R T_R} \qquad \textbf{Eq. H}$$

which is Eq. 15.

## APPENDIX E. KUTATELADZE EQUATION CORRECTION

The following is Randall F. Barron's explanation of the presentation of the Kutateladze equation in his book, *Cryogenic Heat Transfer.* The material was sent by Mr. Barron directly to the KSC Engineering Design Analysis Branch on June 5, 2008. Mr. Barron's work has been typeset and lightly edited for consistency.

**Table 8. Comparison of Symbols**

| Kutateladze | *Cryogenic Heat Transfer* | Kutateladze Equation Units |
|---|---|---|
| $\frac{\upsilon}{a}$, Prandtl number of liquid | $\mathrm{Pr}_L = \frac{\mu_L c_L}{k_L}$ | dimensionless |
| $\upsilon$, kinematic viscosity | $\frac{\mu_L}{\rho_L}$ | $m^2/s$ |
| $a$, thermal diffusivity | $\frac{k_L}{\rho_L c_L}$ | $m^2/s$ |
| $q$, boiling heat flux | $\frac{Q}{A_W}$ | $W/m^2$ |
| $r$, latent heat of vaporization | $i_{fg}\left(\frac{g_c}{g}\right)$ | $J/kg_f$ |
| $\sigma$, surface tension | $\sigma_L$ | $kg_f/m$ |
| $\gamma$, specific weight of liquid | $\frac{\rho_L g}{g_c}$ | $kg_f/m^3$ |
| $\gamma$", specific weight of vapor | $\frac{\rho_G g}{g_c}$ | $kg_f/m^3$ |
| $\alpha$, boiling coefficient | $h_b = \frac{Q}{A_W \cdot \Delta T}$ | $W/m^2 \cdot °C$ |
| $\lambda$, thermal cond. of liquid | $k_L$ | $W/m \cdot °C$ |
| $\frac{c \cdot \Delta T}{r}$ | $J_a = \frac{c_L \Delta T}{i_{fg}}$, Jakob number | dimensionless |
| $\frac{p}{\sqrt{\sigma(\gamma - \gamma")}}$ | $K_P = \frac{P_{SAT}}{\sqrt{(g/g_c)\sigma_L(\rho_L - \rho_G)}}$ | dimensionless |
| $(0.44)(10^{-4})^{0.7}$ | $6.9735\times10^{-4} \approx 7.0\times10^{-4}$ | |

**NOTE**

> Russian scientists often used a "gravimetric" metric system, based on mass (in kilograms [kg]), length (in meters [m]), time (in seconds [s]), and force (in kilograms [kgf]). The conversion factor between SI and the other metric unit for force is 9.807 newtons per kilogram of force (N/kgf).

Beginning with the Kutateladze equation in the Kutateladze-notation,

$$\frac{\alpha}{\lambda}\sqrt{\frac{\sigma}{\gamma-\gamma''}} = 0.44\left(\frac{\upsilon}{a}\right)^{0.35}\left[\frac{q}{r\gamma''\upsilon}\sqrt{\frac{\sigma}{\gamma-\gamma''}}\right]^{0.7}\left[\frac{p\times 10^{-4}}{\sqrt{\sigma(\gamma-\gamma'')}}\right]^{0.7}$$

Converting to the notation used in *Cryogenic Heat Transfer* (as given in Table 8), the Kutateladze equation may be written as follows:

$$\frac{(Q/A_W)}{k_L\Delta T}\sqrt{\frac{g_c\sigma_L}{g(\rho_L-\rho_G)}} = 7.0\times 10^{-4}\,\mathrm{Pr}_L^{0.35}\left[\frac{(Q/A_W)\rho_L}{i_{fg}\mu_L\rho_G}\sqrt{\frac{g_c\sigma_L}{g(\rho_L-\rho_G)}}\right]^{0.7}\left[\frac{P}{\sqrt{(g/g_c)(\rho_L-\rho_G)}}\right]^{0.7}$$

Introducing $k_L = \mu_L c_L/\mathrm{Pr}_L$, moving the density ratio $(\rho_L/\rho_G)$ into the second bracketed term, and multiplying and dividing by $i_{fg}$ on the left side yields

$$\frac{\mathrm{Pr}_L\, i_{fg}}{c_L\Delta T}\left[\frac{(Q/A_W)}{i_{fg}\mu_L}\sqrt{\frac{g_c\sigma_L}{g(\rho_L-\rho_G)}}\right] = 0.0007\,\mathrm{Pr}_L^{0.35}\left[\frac{(Q/A_W)}{i_{fg}\mu_L}\sqrt{\frac{g_c\sigma_L}{g(\rho_L-\rho_G)}}\right]^{0.7}\left[\frac{\rho_L P}{\rho_G\sqrt{(g/g_c)(\rho_L-\rho_G)}}\right]^{0.7}$$

Introducing the Jakob number, $J_a = c_L\Delta T/i_{fg}$, on the left side, dividing through by $\mathrm{Pr}_L^{0.35}$, and dividing through by the first bracketed term on the right side yields

$$\frac{\mathrm{Pr}_L^{0.65}}{J_a}\left[\frac{(Q/A_W)}{i_{fg}\mu_L}\sqrt{\frac{g_c\sigma_L}{g(\rho_L-\rho_G)}}\right]^{0.3} = 0.0007\left[\frac{\rho_L P}{\rho_G\sqrt{(g/g_c)(\rho_L-\rho_G)}}\right]^{0.7}$$

Introducing on the right side the definition of the factor $K_P$, defined by

$$K_P = \frac{P_{SAT}}{\sqrt{(g/g_c)\sigma_L(\rho_L-\rho_G)}}$$

yields

$$\frac{\Pr_L^{0.65}}{J_a}\left[\frac{(Q/A_W)}{i_{fg}\mu_L}\sqrt{\frac{g_c\sigma_L}{g(\rho_L-\rho_G)}}\right]^{0.3} = 0.0007\left[\frac{\rho_L K_P}{\rho_G}\right]^{0.7}$$

Solving for the Jakob number, $J_a$,

$$\frac{J_a}{\Pr_L^{0.65}} = \frac{1}{0.0007}\left[\frac{(Q/A_W)}{i_{fg}\mu_L}\sqrt{\frac{g_c\sigma_L}{g(\rho_L-\rho_G)}}\right]^{0.3}\left[\frac{\rho_G}{\rho_L K_P}\right]^{0.7}$$

This is the correct form for Equation 4-24, pg. 164, *Cryogenic Heat Transfer*. In the correct form, the factor 0.0007 and $K_P$ shall be in the denominator, instead of the numerator. The equation was written in this form so that the Kutateladze equation could be compared with the Rohsenow equation,

$$\frac{J_a}{\Pr_L^{n}} = C_{sf}\left[\frac{(Q/A_W)}{i_{fg}\mu_L}\sqrt{\frac{g_c\sigma_L}{g(\rho_L-\rho_G)}}\right]^{1/3}$$

a. In the Kutateladze equation, $n$ = 0.65 for all fluids; in the Rohsenow equation, $n$ = 1 for water and $n$ = 1.7 for all other fluids.

b. In the Kutateladze equation, the exponent on the term containing the heat flux ($Q/A_W$) is 0.300; in the Rohsenow equation, the corresponding exponent is $^1/_3$ = 0.333.

c. The surface-fluid coefficient $C_{sf}$ in the Rohsenow equation is a constant for a particular surface-fluid combination, independent of the fluid pressure. In the Kutateladze equation, the corresponding factor does not involve the surface-fluid combination; however, there is pressure dependence.

$$\frac{1}{0.0007}\left[\frac{\rho_G\sqrt{(g/g_c)(\rho_L-\rho_G)}}{\rho_L P_{SAT}}\right]^{0.7}$$ corresponds to $C_{sf}$ in the Rohsenow equation.

This is generally not an extremely strong pressure-dependent term, because $\rho_G$ is also pressure-dependent, and the ratio ($\rho_G/P_{SAT}$) does not vary by orders of magnitude with pressure.

- At 1 atmosphere (atm) = 101.3 kPa (14.69 psia), $(\rho_G/P_{SAT})^{0.7} = (4.604/101.3)^{0.7}$ = 0.1149.

- At 1.349 atm = 136.7 kPa (19.83 psia), $(\rho_G/P_{SAT})^{0.7} = (6.071/136.7)^{0.7}$ = 0.1130.

- At 2 atm = 202.6 kPa (29.38 psia), $(\rho_G/P_{SAT})^{0.7} = (8.753/202.6)^{0.7} = 0.1109$.

For saturated liquid nitrogen boiling at 80 K (–193.2 °C = –315.7 °F = 144 °R), we find the following physical properties:

| **In *Cryogenic Heat Transfer*** | **In Kutateladze** |
|---|---|
| $\Pr_L$ = 2.14 | $\upsilon/a$ = 2.14 |
| $(Q/A_W)$ = 3154 W/m$^2$ (1000 Btu/hr·ft$^2$) | $q$ = 3154 W/m$^2$ |
| $i_{fg}$ = 195.8 kJ/kg (84.2 Btu/lb$_m$) | $r$ = 195.8 kJ/kg$_f$ |
| $\sigma_L$ = 8.22 mN/m (0.563×10$^{-3}$ lb$_f$/ft) | $\sigma$ = 0.838×10$^{-3}$ kg$_f$/m |
| $\rho_L$ = 795.1 kg/m$^3$ (49.64 lb$_m$/ft$^3$) | $\gamma$ = 795.1 kg$_f$/m$^3$ |
| $\rho_G$ = 6.071 kg/m$^3$ (0.379 lb$_m$/ft$^3$) | $\gamma''$ = 6.071 kg$_f$/m$^3$ |
| $k_L$ = 0.1362 W/m·°C (0.0787 Btu/hr·ft·°F) | $\lambda$ = 0.1362 W/m·°C |
| $c_L$ = 2.063 kJ/kg·°C (0.493 Btu/lb$_m$·°F) | |
| $\mu_L$ = 141 $\mu$Pa·s (0.341 lb$_m$/ft·hr) | |
| | $\upsilon$ = 0.1773 mm$^2$/s |
| $p_{sat}$ = 136.7 kPa (19.83 psia) | $p$ = 13,939 kg$_f$/m$^2$ |
| $g$ = 9.807 m/s$^2$ (32.174 ft/s$^2$) | $g$ = 9.807 m/s$^2$ |
| $g_c$ = 1 kg·m/N·s$^2$ (32.174 lb$_m$·ft/lb$_f$·s$^2$) | $g_c$ = 9.807 kg$_m$/kg$_f$·s$^2$ |

Using these properties, we may calculate the temperature difference, $\Delta T = T_W - T_{SAT}$, for liquid nitrogen in pool boiling at 136.7 kPa (19.83 psia or 1.349 atm) and 80 K (315.67 °F), using the original Kutateladze equation and the form presented in *Cryogenic Heat Transfer* (corrected). We find that these two calculations result in the same temperature difference.

The form presented in *Cryogenic Heat Transfer* separates the term involving $\Delta T$ and the term involving $(Q/A_W)$. Because the heat flux term appears (implicitly) in $\alpha = (Q/A_W)/\Delta T$ and also in the first term on the right side, the solution for the heat flux is somewhat more awkward using Kutateladze's original formulation.

**Calculation of Δ*T* – Kutateladze's Original Equation Form**

$$\frac{q}{r\gamma''\upsilon}\left(\frac{\sigma}{\gamma-\gamma''}\right)^{1/2} = \frac{(3154)}{(195.8\times10^{3})(6.071)(0.1773\times10^{-6})}\left(\frac{0.838\times10^{-3}}{795.1-6.071}\right)^{1/2} = 15.423$$

$$K_P = \frac{p}{\sqrt{\sigma(\gamma-\gamma'')}} = \frac{13{,}939}{\sqrt{(0.838\times10^{-3})(795.1-6.071)}} = 17{,}140$$

The left side of the original Kutateladze equation is a form of a "boiling Nusselt number,"

$$\frac{\alpha}{\lambda}\sqrt{\frac{\sigma}{\gamma-\gamma''}} = (0.44)(2.14)^{0.35}(15.423)^{0.7}(17{,}142\times10^{-4})^{0.7} = 5.6840$$

The boiling heat transfer coefficient is

$$\alpha = \frac{(5.6840)(0.1362)}{\sqrt{(0.838\times10^{-3})/(795.1-6.071)}} = \frac{(5.6840)(0.1362)}{(0.0010306)} = 751.2\ \mathrm{W/m^2\cdot{}^\circ C} = \frac{(Q/A_W)}{\Delta T}$$

The temperature difference, according to the original Kutateladze equation, is

$$\Delta T = \frac{3154}{751.2} = 4.20\ {}^\circ\mathrm{C} = T_W - T_{SAT} \Leftarrow$$

**Calculation of ΔT – Kutateladze's Equation in *Cryogenic Heat Transfer* Form**

$$\frac{(Q/A_W)}{i_{fg}\mu_L}\sqrt{\frac{g_c\sigma_L}{g(\rho_L-\rho_G)}} = \frac{(3154)}{(195.8\times10^{3})(141\times10^{-6})}\sqrt{\frac{(1)(8.22\times10^{-3})}{(9.807)(795.1-6.071)}} = 0.11775$$

$$K_P = \frac{P_{SAT}}{\sqrt{(g/g_c)\sigma_L(\rho_L-\rho_G)}} = \frac{(136.7\times10^{3})}{\sqrt{(9.807/1)(8.22\times10^{-3})(795.1-6.071)}} = 17{,}140$$

The Jakob number is

$$J_a = \frac{(2.14)^{0.65}}{(0.0007)}(0.11775)^{0.3}\left[\left(\frac{6.071}{795.1}\right)\frac{1}{17{,}140}\right]^{0.7} = 0.04417 = \frac{c_L\Delta T}{i_{fg}}$$

$$\Delta T = \frac{(0.04417)(195.8\times10^{3})}{(2.063\times10^{3})} = 4.20\ {}^\circ\mathrm{C} \Leftarrow$$

For comparison, we can determine the temperature difference $\Delta T$ using the Rohsenow equation for nucleate boiling:

$$\frac{J_a}{\mathrm{Pr}_L^{1.7}} = C_{sf}\left[\frac{(Q/A_w)}{i_{fg}\mu_L}\sqrt{\frac{g_c\sigma_L}{g(\rho_L-\rho_G)}}\right]^{1/3}$$

Using a value of $C_{sf} = 0.013$, we find the Jakob number, according to the Rohsenow equation:

$J_a = (0.013)(2.14)^{1.7}\,(0.11775)^{1/3} = 0.02323$

The temperature difference is

$$\Delta T = \frac{(0.02323)(195.8)}{(2.063)}$$ = 2.20 °C (compared to 4.20 °C from the Kutateladze equation)

The experimentally measured temperature difference for liquid nitrogen with a boiling heat flux of $(Q/A_W) = 3154\ \mathrm{W/m^2} = 0.3154\ \mathrm{W/cm^2}$ is $\Delta T = 3.2$ °C.

See [15].

The differences between calculated and experimental values are

- (4.2 °C – 3.2 °C)/(3.2 °C) = +31% (for the Kutateladze equation) and
- (2.2 °C – 3.2 °C)/(3.2 °C) = –31% (for the Rohsenow equation).

# APPENDIX F. PNEUMATIC RELIEF VALVE SIZING

## F.1 No Upstream Loss Case

### F.1.1 Relief Valve Sizing, Part 1

To size a relief valve set at or below system design pressure to relieve flow from a failed regulator in AFT Arrow or similar software, assuming no losses upstream of the regulator:

1) Use Maximum Expected Inlet Supply Pressure
2) Use Minimum Expected Inlet Supply Temperature
3) Remove all non-flowpath-related pipe/tubing and components (simplify the model) Note: all of the Failed Regulator Flow is to pass through the subject Relief Valve
4) Remove Losses (including embedded losses) between Inlet Supply and Failed Regulator Inlet. Do not use "frictionless" pipes/tubes. Instead shorten the lengths of these upstream tubes to 0.1"
5) Use Maximum CdA Value of Orifice (if it exists) Upstream of Regulator. Reference GP-425 if applicable.
6) Configure Regulator to be Failed Fully Open (No Control)
7) Use an Assigned Pressure Junction at the Relief Valve location with Stagnation Pressure (PSIG) at R/V Set Pressure at upper "high flow" Pressure tolerance of +/- 3% above R/V Set Pressure or +/- 2 PSIG above R/V Set Pressure, whichever pressure is greater.
8) Run the case.

Once the case has run, verify the following:

- Supply pressure is projected at the inlet to the failed regulator.
- Pressure at failed regulator exit is no more than 110% of system design pressure.
- Relief valve relieves within tolerances specified by ASME Section VIII Div. 1 paragraph UG-126(c) (+/-3% of RV set pressure or +/- 2 psig, whichever is greater). RV set pressure in the model may have to be set to tolerance boundaries manually to ensure adequate system performance.

### F.1.2 Relief Valve Sizing, Part 2

To determine the R/V Flow Capacity using AFT Arrow or similar software:

1) Determine the R/V Flow Capacity and compare to Failed Regulator Flowrate (as referenced above).

2) Shorten R/V inlet pipe/tube length to 0.1” and remove any embedded piping losses. Do not use “frictionless” pipes/tubes.
3) Set the Inlet Stagnation Pressure at upper “high flow” pressure tolerance of +/- 3% above R/V Set Pressure or +/- 2 PSIG above R/V Set Pressure, whichever pressure is greater
4) Use an Inlet Stagnation Temperature of 120 ºF
5) Model R/V with R/V Orifice CdA for Sonic Choking and select Exit to Atmosphere
6) Fail the R/V open.
7) Run the case and capture the Mass Flowrate
8) Verify that R/V Flow Capacity > Failed Regulator Flowrate

### F.1.3 Relief Valve Sizing, Part 3

To determine the R/V Captured Vent System Back Pressure using AFT Arrow or similar software:

1) Determine the Failed Regulator Flowrate (as referenced above).
2) Use an Assigned Flowrate Junction at the R/V Exit location and as an input into the model Vent System
3) Set the Inlet Static Temperature at T = 120ºF
4) Set the Vent System Exit Pressure to P = 14.696 PSIA
5) Run the case and capture the calculated Inlet Stagnation Pressure at the Assigned Flowrate Junction
6) Verify that Inlet Stagnation Pressure (PSIG) ≤ R/V Set Pressure (PSIG) x 0.10

Notes:

- In the rare but possible case of two relief valves supporting a single failed regulator, where the two relief valves are at different set pressures, one should be concerned as to the possible pressure accumulation upstream of the relief valve with the lower set pressure for the time duration until the second relief valve with the higher set pressure is activated. This may require a gas transient analysis and is a function of the tube internal volumes, the flowrate through the failed regulator, the respective relief valve set pressures and flow capacities of those relief valves and the proximity location of the relief valves to each other and the failed regulator.
- ASME Boiler Pressure Vessel Code Section VIII Div 1 Part M-7 (2015) indicates that the pressure limit in the vent header (downstream of the Relief Valve) should be less than 10% of the Relief Valve Set Pressure. This pressure limit is STATIC PRESSURE. Utilizing stagnation pressure is conservative as the stagnation minus the dynamic pressure is static pressure. If the internal diameters associated with these pressures is known, then the static pressure may be calculated and used for this comparison.

However, the stagnation pressure is conservative and does not require the internal diameters to be known and if the system passes using stagnation pressures then it should also be acceptable for static pressures.

## F.2 All Upstream Loss Case

Approach is identical to above, except disregard Part 1 Steps 3 and 4. Configure the model as needed to ensure that all flow through the regulator passes through the subject relief valve.

# STANDARDIZATION DOCUMENT IMPROVEMENT PROPOSAL

INSTRUCTIONS

1. The preparing activity must complete blocks 1, 2, 3, and 8. In block 1, both the document number and revision letter should be given.
2. The submitter of this form must complete blocks 4, 5, 6, and 7.
3. The preparing activity must provide a reply within 30 days from receipt of the form.

NOTE: This form may not be used to request copies of documents, nor to request waivers or clarification of requirements on current contracts. Comments submitted on this form do not constitute or imply authorization to waive any portion of the referenced document or to amend contractual requirements.

| **I RECOMMEND A CHANGE:** | 1. DOCUMENT NUMBER<br>KSC-STD-Z-0017 | 2. DOCUMENT DATE<br>September 7, 20 |
|---|---|---|

3. DOCUMENT TITLE
Engineering Analysis, Thermal/Fluid,
Standard For

4. NATURE OF CHANGE *(Identify paragraph number and include proposed rewrite, if possible. Attach extra sheets as needed.)*

5. REASON FOR RECOMMENDATION

**6. SUBMITTER**

| a. NAME *(Last, First, Middle Initial)* | b. ORGANIZATION | |
|---|---|---|
| c. ADDRESS *(Include Zip Code)* | d. TELEPHONE *(Include Area Code)* | 7. DATE SUBMITTED |

**8. PREPARING ACTIVITY**

| a. NAME | b. ORGANIZATION |
|---|---|
| Craig Fortier | Engineering Analysis Branch |

c. ADDRESS *(Include Zip Code)*
Mail Stop NE-XY, Kennedy Space Center, Florida 32899